
**Calculation of scuffing load capacity of
cylindrical, bevel and hypoid gears —**

**Part 2:
Integral temperature method**

*Calcul de la capacité de charge au grippage des engrenages cylindriques,
coniques et hypoides —*

Partie 2: Méthode de la température intégrale



Reference number
ISO/TR 13989-2:2000(E)

© ISO 2000

PDF disclaimer

This PDF file may contain embedded typefaces. In accordance with Adobe's licensing policy, this file may be printed or viewed but shall not be edited unless the typefaces which are embedded are licensed to and installed on the computer performing the editing. In downloading this file, parties accept therein the responsibility of not infringing Adobe's licensing policy. The ISO Central Secretariat accepts no liability in this area.

Adobe is a trademark of Adobe Systems Incorporated.

Details of the software products used to create this PDF file can be found in the General Info relative to the file; the PDF-creation parameters were optimized for printing. Every care has been taken to ensure that the file is suitable for use by ISO member bodies. In the unlikely event that a problem relating to it is found, please inform the Central Secretariat at the address given below.

© ISO 2000

All rights reserved. Unless otherwise specified, no part of this publication may be reproduced or utilized in any form or by any means, electronic or mechanical, including photocopying and microfilm, without permission in writing from either ISO at the address below or ISO's member body in the country of the requester.

ISO copyright office
Case postale 56 • CH-1211 Geneva 20
Tel. + 41 22 749 01 11
Fax + 41 22 734 10 79
E-mail copyright@iso.ch
Web www.iso.ch

Printed in Switzerland

Contents

Page

Foreword.....	v
Introduction	vi
1 Scope	1
2 Normative references	1
3 Terms, definitions, symbols and units	1
3.1 Terms and definitions	1
3.2 Symbols and units	1
4 Field of application	6
4.1 Scuffing damage	6
4.2 Integral temperature criterion.....	7
5 Influence factors	7
5.1 Mean coefficient of friction μ_{mC}	7
5.2 Run-in factor X_E	10
5.3 Thermal flash factor X_M	10
5.4 Pressure angle factor $X_{\alpha\beta}$	11
6 Calculation.....	12
6.1 Cylindrical gears.....	12
6.1.1 Scuffing safety factor S_{intS}	12
6.1.2 Permissible integral temperature ϑ_{intP}	12
6.1.3 Integral temperature ϑ_{int}	12
6.1.4 Flash temperature at pinion tooth tip ϑ_{flaE}	13
6.1.5 Bulk temperature ϑ_M	13
6.1.6 Mean coefficient of friction μ_{mC}	14
6.1.7 Run-in factor X_E	14
6.1.8 Thermal flash factor X_M	14
6.1.9 Pressure angle factor $X_{\alpha\beta}$	14
6.1.10 Geometry factor at tip of pinion X_{BE}	14
6.1.11 Approach factor X_Q	14
6.1.12 Tip relief factor X_{Ca}	15
6.1.13 Contact ratio factor: X_ε	16
6.2 Bevel gears.....	19
6.2.1 Scuffing safety factor S_{intS}	20
6.2.2 Permissible integral temperature ϑ_{intP}	20
6.2.3 Integral temperature ϑ_{int}	20
6.2.4 Flash temperature at pinion tooth tip ϑ_{flaE}	20
6.2.5 Bulk temperature ϑ_M	20
6.2.6 Mean coefficient of friction μ_{mC}	20
6.2.7 Run-in factor X_E	21
6.2.8 Thermal flash factor X_M	21
6.2.9 Pressure angle factor $X_{\alpha\beta}$	21
6.2.10 Geometry factor at tip of pinion X_{BE}	21
6.2.11 Approach factor X_Q	21
6.2.12 Tip relief factor X_{Ca}	21
6.2.13 Contact ratio factor X_ε	22

6.3	Hypoid gears	22
6.3.1	Scuffing safety factor S_{intS}	22
6.3.2	Permissible integral temperature ϑ_{intP}	22
6.3.3	Integral temperature ϑ_{int}	22
6.3.4	Bulk temperature ϑ_M	22
6.3.5	Mean coefficient of friction μ_{mC}	23
6.3.6	Run-in factor X_E	23
6.3.7	Geometry factor X_G	23
6.3.8	Approach factor X_Q	24
6.3.9	Tip relief factor X_{Ca}	25
6.3.10	Contact ratio factor X_ε	25
6.3.11	Calculation of virtual crossed axes helical gears	25
6.4	Scuffing integral temperature	29
6.4.1	Scuffing integral temperature ϑ_{intS}	29
6.4.2	Relative welding factor X_{WrelT}	33
Annex A (informative) Examples		34
Annex B (informative) Contact-time-dependent scuffing temperature		44
Bibliography		48

www.iso.org

Foreword

ISO (the International Organization for Standardization) is a worldwide federation of national standards bodies (ISO member bodies). The work of preparing International Standards is normally carried out through ISO technical committees. Each member body interested in a subject for which a technical committee has been established has the right to be represented on that committee. International organizations, governmental and non-governmental, in liaison with ISO, also take part in the work. ISO collaborates closely with the International Electrotechnical Commission (IEC) on all matters of electrotechnical standardization.

The main task of technical committees is to prepare International Standards, but in exceptional circumstances a technical committee may propose the publication of a Technical Report of one of the following types:

- type 1, when the required support cannot be obtained for the publication of an International Standard, despite repeated efforts;
- type 2, when the subject is still under technical development or where for any other reason there is the future but not immediate possibility of an agreement on an International Standard;
- type 3, when a technical committee has collected data of a different kind from that which is normally published as an International Standard ("state of the art", for example).

Technical Reports of types 1 and 2 are subject to review within three years of publication, to decide whether they can be transformed into International Standards. Technical Reports of type 3 do not necessarily have to be reviewed until the data they provide are considered to be no longer valid or useful.

Technical Reports are drafted in accordance with the rules given in the ISO/IEC Directives, Part 3.

Attention is drawn to the possibility that some of the elements of this part of ISO/TR 13989 may be the subject of patent rights. ISO shall not be held responsible for identifying any or all such patent rights.

ISO/TR 13989-2, which is a Technical Report of type 2, was prepared by Technical Committee ISO/TC 60, *Gears*, Subcommittee SC 2, *Gear capacity calculation*.

This document is being issued in the Technical Report (type 2) series of publications (according to subclause G.3.2.2 of Part 1 of the ISO/IEC Directives, 1995) as a "prospective standard for provisional application" in the field of scuffing load capacity of gears because there is an urgent need for guidance on how standards in this field should be used to meet an identified need. In 1975, two methods to evaluate the risk of scuffing were documented to be studied by ISO/TC 60. It was agreed that after a period of experience one method shall be selected. Since the subject is still under technical development and there is a future possibility of an agreement on an International Standard, the publication of a type 2 Technical Report was proposed.

This document is not to be regarded as an "International Standard". It is proposed for provisional application so that information and experience of its use in practice may be gathered. Comments on the content of this document should be sent to the ISO Central Secretariat.

A review of this Technical Report (type 2) will be carried out not later than three years after its publication with the options of: extension for another three years; conversion into an International Standard; or withdrawal.

ISO/TR 13989 consists of the following parts, under the general title *Calculation of scuffing load capacity of cylindrical, bevel and hypoid gears*:

- *Part 1: Flash temperature method*
- *Part 2: Integral temperature method*

Annexes A and B of this part of ISO/TR 13989 are for information only.

Introduction

This part of ISO/TR 13989 describes the surface damage "warm scuffing" for cylindrical (spur and helical), bevel and hypoid gears for generally used gear materials and different heat treatments. "Warm scuffing" is characterized by typical scuffing and scoring marks, which can lead to increasing power loss, dynamic load, noise and wear. For "cold scuffing", in general associated with low temperature and low speed, under approximately 4 m/s, and through-hardened, heavily loaded gears, the equations are not suitable.

There is a particularly severe form of gear tooth surface damage in which seizure or welding together of areas of tooth surfaces occurs, due to absence or breakdown of a lubricant film between the contacting tooth flanks of mating gears, caused by high temperature and high pressure. This form of damage is termed "scuffing" and most relevant when surface velocities are high. Scuffing may also occur for relatively low sliding velocities when tooth surface pressures are high enough, either generally or, because of uneven surface geometry and loading, in discrete areas.

Risk of scuffing damage varies with the properties of gear materials, the lubricant used, the surface roughness of tooth flanks, the sliding velocities and the load. Excessive aeration or the presence of contaminants in the lubricant such as metal particles in suspension, also increase the risk of scuffing damage. Consequences of the scuffing of high speed gears include a tendency to high levels of dynamic loading due to increase of vibration, which usually leads to further damage by scuffing, pitting or tooth breakage.

High surface temperatures due to high surface pressures and sliding velocities can initiate the breakdown of lubricant films. On the basis of this hypothesis two approaches to relate temperature to lubricant film breakdown are presented:

- the flash temperature method (presented in ISO/TR 13989-1), based on contact temperatures which vary along the path of contact;
- the integral temperature method (presented in this part of ISO/TR 13989), based on the weighted average of the contact temperatures along the path of contact.

The integral temperature method is based on the assumption that scuffing is likely to occur when the mean value of the contact temperature (integral temperature) is equal to or exceeds a corresponding critical value. The risk of scuffing of an actual gear unit can be predicted by comparing the integral temperature with the critical value, derived from a gear test for scuffing resistance of lubricants. The calculation method takes account of all significant influence parameters, i.e. the lubricant (mineral oil with and without EP-additives, synthetic oils), the surface roughness, the sliding velocities, the load, etc.

In order to ensure that all types of scuffing and comparable forms of surface damage due to the complex relationships between hydrodynamical, thermodynamical and chemical phenomena are dealt with, further methods of assessment may be necessary. The development of such methods is the objective of ongoing research.

Calculation of scuffing load capacity of cylindrical, bevel and hypoid gears —

Part 2: Integral temperature method

1 Scope

This part of ISO/TR 13989 specifies the integral temperature method for calculating the scuffing load capacity of cylindrical, bevel and hypoid gears.

2 Normative references

The following normative documents contain provisions which, through reference in this text, constitute provisions of this part of ISO/TR 13989. For dated references, subsequent amendments to, or revisions of, any of these publications do not apply. However, parties to agreements based on this part of ISO/TR 13989 are encouraged to investigate the possibility of applying the most recent editions of the normative documents indicated below. For undated references, the latest edition of the normative document referred to applies. Members of ISO and IEC maintain registers of currently valid International Standards.

ISO 53:1998, *Cylindrical gears for general and heavy engineering — Standard basic rack tooth profile*.

ISO 1122-1:1998, *Vocabulary of gear terms — Part 1: Definitions related to geometry*.

ISO 1328-1:1995, *Cylindrical gears — ISO system of accuracy — Part 1: Definitions and allowable values of deviations relevant to corresponding flanks of gear teeth*.

ISO 6336-1:1996, *Calculation of load capacity of spur and helical gears — Part 1: Basic principles, introduction and general influence factors*.

ISO 10300-1:—¹⁾, *Calculation of load capacity of bevel gears — Part 1: Introduction and general influence factors*.

3 Terms, definitions, symbols and units

3.1 Terms and definitions

For the purposes of this part of ISO/TR 13989, the terms and definitions given in ISO 1122-1 apply.

3.2 Symbols and units

The symbols used in this part of ISO/TR 13989 are given in Table 1.

1) To be published.

Table 1 — Symbols and units

Symbol	Description	Unit	Reference
a	centre distance	mm	—
a_v	virtual centre distance of virtual cylindrical gear	mm	ISO 10300-1
b	face width, smaller value of pinion or wheel	mm	—
b_{eB}	effective facewidth for scuffing	mm	Eq. (46)
c_v	specific heat capacity per unit volume	N/(mm ² ·K)	—
c'	single stiffness	N/(mm·μm)	ISO 6336-1
c_γ	mesh stiffness	N/(mm·μm)	ISO 6336-1
d	reference circle diameter	mm	—
d_{Na}	effective tip diameter	mm	—
d_a	tip diameter	mm	Eq. (69)
d_b	base diameter	mm	Eq. (70)
d_m	diameter at mid-facewidth	mm	—
d_s	reference circle of virtual crossed axes helical gear	mm	Eq. (68)
d_v	reference diameter of virtual cylindrical gear	mm	ISO 10300-1
d_{va}	tip diameter of virtual cylindrical gear	mm	ISO 10300-1
d_{vb}	base diameter of virtual cylindrical gear	mm	ISO 10300-1
$g_{an1,2}$	recess path of contact of pinion, wheel	mm	Eqs. (90), (91)
$g_{fn1,2}$	approach path of contact of pinion, wheel	mm	Eqs. (90), (91)
g^*	sliding factor	—	Eq. (62)
h_{am}	addendum at mid-facewidth of hypoid gear	mm	—
m	module	mm	—
m_{mn}	normal module of hypoid gear at mid-facewidth	mm	—
m_{sn}	normal module of virtual crossed axes helical gear	mm	Eq. (73)
n_p	number of meshing gears	—	—
p_{en}	normal base pitch	mm	Eq. (74)
u	gear ratio	—	—
u_v	gear ratio of virtual cylindrical gear	—	ISO 10300-1
v	reference line velocity	m/s	—
$v_{t1,2}$	tangential velocity of pinion, wheel of hypoid gear	m/s	Eqs. (77), (78)
$v_{g\gamma 1}$	maximum sliding velocity at tip of pinion	m/s	Eq. (83)
v_{gs}	sliding velocity at pitch point	m/s	Eq. (82)
$v_{g1,2}$	sliding velocity	m/s	Eqs. (84), (85)
$v_{g\alpha 1}$	sliding velocity	m/s	Eq. (87)

Table 1 (continued)

Symbol	Description	Unit	Reference
$v_{g\beta 1}$	sliding velocity	m/s	Eq. (88)
v_{mt}	tangential speed at reference cone at mid-facewidth of bevel gear	m/s	—
$v_{\Sigma C}$	sums of tangential speeds at pitch point	m/s	Eqs. (2), (47), (81)
$v_{\Sigma S}$	tangential speed	m/s	Eq. (79)
$v_{\Sigma h}$	tangential speed	m/s	Eq. (80)
w_{Bt}	specific tooth load, scuffing	N/mm	Eq. (4)
z	number of teeth	—	—
z_v	number of teeth of virtual cylindrical gear	—	ISO 10300-1
B_M	thermal contact coefficient	N/(mm·s ^{1/2} ·K)	Eq. (12)
C_1, C_2, C_{2H}	weighting factors	—	—
C_a	nominal tip relief	μm	—
C_{eff}	effective tip relief	μm	Eqs. (37), (38), (49)
E	module of elasticity (Young's modulus)	N/mm ²	—
F_{mt}	nominal tangential load at reference cone at mid-facewidth	N	—
F_n	normal tooth load	N	Eq. (51)
F_t	nominal tangential load at reference circle	N	—
K_A	application factor	—	ISO 6336-1, ISO 10300-1
K_V	dynamic factor	—	ISO 6336-1, ISO 10300-1
$K_{B\alpha}$	= $K_{H\alpha}$ transverse load factor (scuffing)	—	6.2.4, ISO 6336-1, ISO 10300-1
$K_{B\beta}$	= $K_{H\beta}$ face load factor (scuffing)	—	ISO 6336-1, ISO 10300-1, 6.2.4, Eqs. (52), (53)
$K_{B\gamma}$	helical load factor (scuffing)	—	Eq. (5), 6.2.4, 6.3.5
$K_{B\beta be}$	bearing factor	—	6.3.3
$K_{H\alpha}$	transverse load factor	—	ISO 6336-1, ISO 10300-1
$K_{H\beta}$	face load factor	—	ISO 6336-1, ISO 10300-1
$K_{H\beta be}$	bearing factor	—	ISO 10300-1
L	contact parameter	—	Eq. (55)
R_a	arithmetic mean roughness	μm	Eq. (6)
S_{intS}	scuffing safety factor	—	Eq. (14)
S_{Smin}	minimum required scuffing safety factor	—	—

Table 1 (continued)

Symbol	Description	Unit	Reference
T_1	torque of the pinion	Nm	—
T_{1T}	scuffing torque of test pinion	Nm	Eq. (96)
X_{BE}	geometry factor at pinion tooth tip	—	Eq. (22)
X_E	run-in factor	—	Eq. (8)
X_{Ca}	tip relief factor	—	Eq. (32)
X_G	geometry factor of hypoid gears	—	Eq. (54)
X_L	lubricant factor	—	5.1
X_M	thermal flash factor	—	Eq. (9)
X_Q	approach factor	—	Eqs. (25), (26), (27)
X_R	roughness factor	—	Eq. (7)
X_S	lubrication factor	—	6.1.5.3
X_W	welding factor of executed gear	—	Table 3
X_{WT}	welding factor of test gear	—	6.4.2
X_{WrelT}	relative welding factor	—	Eq. (102)
X_{mp}	contact factor	—	Eq. (21)
$X_{\alpha\beta}$	pressure angle factor	—	Eqs. (13), (48)
X_ε	contact ratio factor	—	Eqs. (39) to (44)
α	pressure angle	°	—
α_{mn}	normal pressure angle at mid-facewidth of hypoid gear	°	—
α_n	normal pressure angle	°	—
α_{sn}	normal pressure angle of crossed axes helical gear	°	Eq. (64)
α_{st}	transverse pressure angle of crossed axes helical gear	°	Eq. (66)
α_t	transverse pressure angle	°	—
α_t'	transverse working pressure angle	°	—
α_{vt}	transverse pressure angle of virtual cylindrical gear	°	ISO 10300-1
α_y	arbitrary angle	°	Figure 2
β	helix angle	°	—
β_b	helix angle at base circle	°	Eqs. (67), (71)
β_m	helix angle at reference cone at mid-facewidth of hypoid gear	°	—
β_s	helix angle of virtual crossed axes helical gear	°	Eq. (63)
γ	auxiliary angle	°	Eq. (86)
δ	reference cone angle	°	—

Table 1 (continued)

Symbol	Description	Unit	Reference
ε_a	recess contact ratio	—	Eqs. (28), (29)
ε_f	approach contact ratio	—	Eqs. (28), (29)
ε_n	contact ratio in normal section of virtual crossed axes helical gear	—	Eqs. (92), (93)
ε_1	addendum contact ratio of the pinion	—	Eq. (30)
ε_2	addendum contact ratio of the wheel	—	Eq. (31)
ε_α	contact ratio	—	Eq. (45)
$\varepsilon_{v\alpha}$	transverse contact ratio of virtual cylindrical gear	—	ISO 10300-1
ε_{v1}	tip contact ratio of virtual cylindrical pinion	—	ISO 10300-1
ε_{v2}	tip contact ratio of virtual cylindrical wheel	—	ISO 10300-1
ξ	Hertzian auxiliary coefficient	—	Figure 7, Eqs. (57), (59)
μ_{mC}	mean coefficient of friction	—	Eqs. (1), (1a)
η_{oil}	dynamic viscosity at oil temperature	mPa·s	—
λ_M	heat conductivity	N/(s·K)	—
ν	Poisson's ratio	—	—
ν_{40}	kinematic viscosity of the oil at 40 °C	mm ² /s; cSt	—
$\rho_{E1,2}$	radius of curvature at tip of the pinion, wheel	mm	Eqs. (23), (24)
ρ_{Cn}	relative radius of curvature at pitch point in normal section	mm	Eq. (76)
$\rho_{n1,2}$	radius of curvature at pitch point in normal section	mm	Eq. (75)
ρ_{redC}	relative radius of curvature at pitch point	mm	Eq. (3)
η	Hertzian auxiliary coefficient	—	Figure 7, Eqs. (58), (60)
ϑ	Hertzian auxiliary angle	°	Eqs. (56) to (60)
ϑ_{flaE}	flash temperature at pinion tooth tip when load sharing is neglected	K	Eq. (19)
ϑ_{flaint}	mean flash temperature	K	Eq. (18)
$\vartheta_{flainth}$	mean flash temperature of hypoid gear	K	Eq. (50)
ϑ_{int}	integral temperature	K	Eq. (17)
ϑ_{intP}	permissible integral temperature	K	Eq. (16)
ϑ_{intS}	scuffing integral temperature (allowable integral temperature)	K	Eq. (94)
$\vartheta_{flaintT}$	mean flash temperature of the test gear	K	Eqs. (96), (99), (101)
ϑ_{oil}	oil sump or spray temperature	°C	—
ϑ_{M-C}	bulk temperature	°C	Eq. (20)

Table 1 (concluded)

Symbol	Description	Unit	Reference
\mathcal{G}_{MT}	test bulk temperature	°C	Eqs. (95), (98), (100)
φ	axle angle of virtual crossed axes helical gear	°	Eq. (72)
Σ	axle angle of virtual crossed axes helical gear	°	Eq. (65)
Φ_E	run-in grade	—	5.2
Γ	parameter on the line of action	—	Eq. (10)

Subscripts:

- 1 pinion
- 2 wheel
- a tip diameter of the virtual gear
- b base circle of the virtual gear
- m mid-facewidth of bevel or hypoid gears
- n normal section
- s virtual crossed axes helical gear
- t tangential direction
- T test gear

4 Field of application

The calculation methods are based on results of the rig testing of gears run at pitch line velocities less than 80 m/s. The equations can be used for gears which run at higher speeds, but with increasing uncertainty as speed increases. The uncertainty concerns the estimation of bulk temperature, coefficient of friction, allowable temperatures, etc. as speeds exceed the range with experimental background.

4.1 Scuffing damage

When once initiated, scuffing damage can lead to gross degradation of tooth flank surfaces, with increase of: power loss, dynamic loading, noise and wear. It can also lead to tooth breakage if the severity of the operating conditions is not reduced. In the event of scuffing due to an instantaneous overload, followed immediately by a reduction of load, e.g. by load redistribution, the tooth flanks may self-heal by smoothing themselves to some extent. Even so, the residual damage will continue to be a cause of increased power loss, dynamic loading and noise.

In most cases, the resistance of gears to scuffing can be improved by using a lubricant with enhanced E.P. (extreme pressure) properties. It is important however, to be aware that some disadvantages attend the use of E.P. oils — corrosion of copper, embrittlement of elastomers, lack of world-wide availability, etc. These disadvantages are to be taken into consideration if optimum lubricant choice is to be made, which means: as few additives as possible, but as many as necessary.

Due to continuous variation of different parameters, the complexity of the chemical properties and the thermo-hydro-elastic processes in the instantaneous contact area, some scatter in the calculated assessments of probability of scuffing risk is to be expected.

In contrast to the relatively long time of development of fatigue damage, one single momentary overload can initiate scuffing damage of such severity that affected gears may no longer be used. This should be carefully considered when choosing an adequate safety factor for gears, especially for gears required to operate at high circumferential velocities.

4.2 Integral temperature criterion

This approach to the evaluation of the probability of scuffing is based on the assumption that scuffing is likely to occur when the mean value of the contact temperatures along the path of contact is equal to or exceeds a corresponding "critical value". In the method presented herein, the sum of the bulk temperature and the weighted mean of the integrated values of flash temperatures along the path of contact is the "integral temperature". The bulk temperature is estimated as described under 6.1.5 and the mean value of the flash temperature is approximated by substituting mean values of the coefficient of friction, the dynamic loading, etc., along the path of contact. A weighting factor is introduced accounting for possible different influences of a real bulk temperature value and a mathematically integrated mean flash temperature value on the scuffing phenomenon.

The probability of scuffing is assessed by comparing the integral temperature with a corresponding critical value derived from the gear testing of lubricants for scuffing resistance (e.g. different FZG test procedures, the IAE and the Ryder gear tests), or from gears which have scuffed in service.

5 Influence factors

5.1 Mean coefficient of friction μ_{mC}

The **actual** coefficient of friction between the tooth flanks is an instantaneous and local value which depends on several properties of the oil, surface roughness, lay of the surface irregularities such as those left by machining, properties of the tooth flank materials, tangential velocities, forces at the surfaces and the dimensions. Assessment of the instantaneous coefficient of friction is difficult since there is no method currently available for its measurement.

The **mean** value for the coefficient of friction μ_{mC} along the path of contact was derived from measurements [1] and approximated by Equation (1). Although the local coefficient of friction is near to zero in the pitch point C, the mean value can be approximated with the parameters at the pitch point and the oil viscosity η_{oil} at oil temperature ϑ_{oil} when introduced into Equation (1).

$$\mu_{mC} = 0,045 \cdot \left(\frac{w_{Bt} \cdot K_{B\gamma}}{v_{\Sigma C} \cdot \rho_{redC}} \right)^{0,2} \cdot \eta_{oil}^{-0,05} \cdot X_R \cdot X_L^2 \quad (1)$$

The coefficient of friction of the integral temperature method takes account of the size of the gear in a different way as the coefficient of friction of the flash temperature method. Equation (1) for calculating the coefficient of friction should not be applied outside the field of the part where it is presented, e.g. coefficient of friction for thermal rating.

The equation for the calculation of μ_{mC} was derived from experiments in the following range of operating conditions. Extrapolation may lead to deviations between the calculated and the real coefficient of friction.

$$1 \text{ m/s} \leq v \leq 50 \text{ m/s}$$

At reference line velocities v lower than 1 m/s, higher coefficients of friction are expected. At reference line velocities v higher than 50 m/s, the limiting value of $v_{\Sigma C}$ at $v = 50$ m/s has to be used in equation (1).

$$w_{Bt} \geq 150 \text{ N/mm}$$

For lower values of the specific normal tooth load w_{Bt} , the limiting value $w_{Bt} = 150$ N/mm has to be used in Equation (1).

$$v_{\Sigma C} = 2 \cdot v \cdot \tan \alpha_t' \cdot \cos \alpha_t \quad (2)$$

$$\rho_{redC} = \frac{u}{(1+u)^2} \cdot a \cdot \frac{\sin \alpha_t'}{\cos \beta_b} \quad (3)$$

$$w_{Bt} = K_A \cdot K_V \cdot K_{B\beta} \cdot K_{B\alpha} \cdot \frac{F_t}{b} \quad (4)$$

2) This formula for the coefficient of friction is derived from testing of gears with centre distance $a \approx 100$ mm.

$$\mu_{mC} = 0,048 \cdot \left(\frac{F_{bt}/b}{v_{\Sigma C} \cdot \rho_{redC}} \right)^{0,2} \cdot \eta_{oil}^{-0,05} \cdot Ra^{0,25} \cdot X_L \quad (1a)$$

where

$$X_L = 0,75 \cdot \left(\frac{6}{v_{\Sigma C}} \right)^{0,2} \quad \text{for polyglycols;}$$

$$X_L = 1,0 \quad \text{for mineral oils;}$$

$$X_L = 0,8 \quad \text{for polyalphaolefins;}$$

$$X_L = 1,5 \quad \text{for traction fluids;}$$

$$X_L = 1,3 \quad \text{for phosphate esters.}$$

Equation (1a) represents results of tests within a range of $a = 91,5$ mm to 200 mm. The application of this equation makes it necessary to adjust Figures 9, 10 and 11 for the scuffing temperature \mathcal{A}_{ntS} accordingly.

$K_{B\gamma}$ is the helical load factor, scuffing takes account of increasing friction for increasing total contact ratio (see Figure 1).

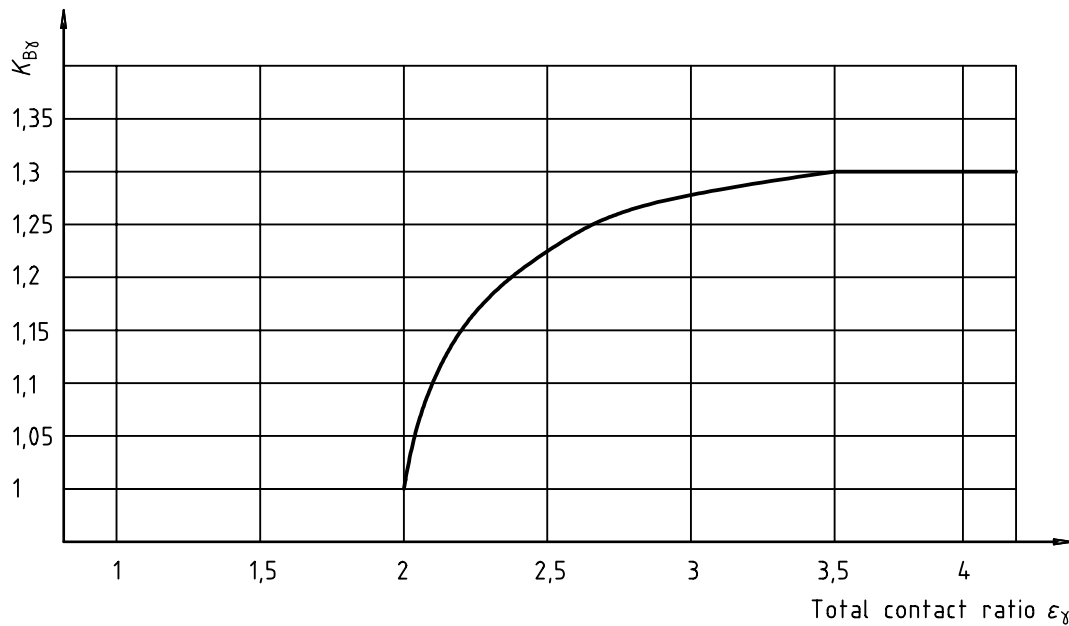


Figure 1 — Helical load factor $K_{B\gamma}$

$$K_{B\gamma} = 1 \quad \text{for } \epsilon_\gamma \leq 2$$

$$K_{B\gamma} = 1 + 0,2 \cdot \sqrt{(\epsilon_\gamma - 2) \cdot (5 - \epsilon_\gamma)} \quad \text{for } 2 < \epsilon_\gamma < 3,5 \quad (5)$$

$$K_{B\gamma} = 1,3 \quad \text{for } \epsilon_\gamma \geq 3,5$$

$$Ra = 0,5 \cdot (Ra_1 + Ra_2) \quad (6)$$

Ra_1 , Ra_2 are the tooth flank roughness values of pinion and wheel measured on the new flanks as manufactured (e.g. reference test gear Ra values are $\approx 0,35 \mu\text{m}$).

$$X_R = 2,2 \cdot (Ra/\rho_{\text{red}C})^{0,25} \quad (7)$$

where

$X_L = 1,0$ for mineral oils;

$X_L = 0,8$ for polyalphaolefins;

$X_L = 0,7$ for non water-soluble polyglycols;

$X_L = 0,6$ for water-soluble polyglycols;

$X_L = 1,5$ for traction fluids;

$X_L = 1,3$ for phosphate esters.

5.2 Run-in factor X_E

The present calculation methods presume that the gears are well run-in. In practice scuffing failure occurs very often during the first few hours in service, e.g. in a full load test run, the acceptance run of vessels or when a new set of gears is built into a production machinery when the gears are run under full load conditions before a proper run-in. Investigations [1] show a 1/4 to 1/3 load carrying capacity of a newly manufactured gear flank as compared to a properly run-in flank. This should be taken into account by a run-in factor X_E :

$$X_E = 1 + (1 - \Phi_E) \cdot \frac{30 \cdot Ra}{\rho_{redC}} \tag{8}$$

where

$\Phi_E = 1$, full run-in (for carburized and ground gears full run-in can be assumed if $Ra_{run-in} \approx 0,6 Ra_{new}$);

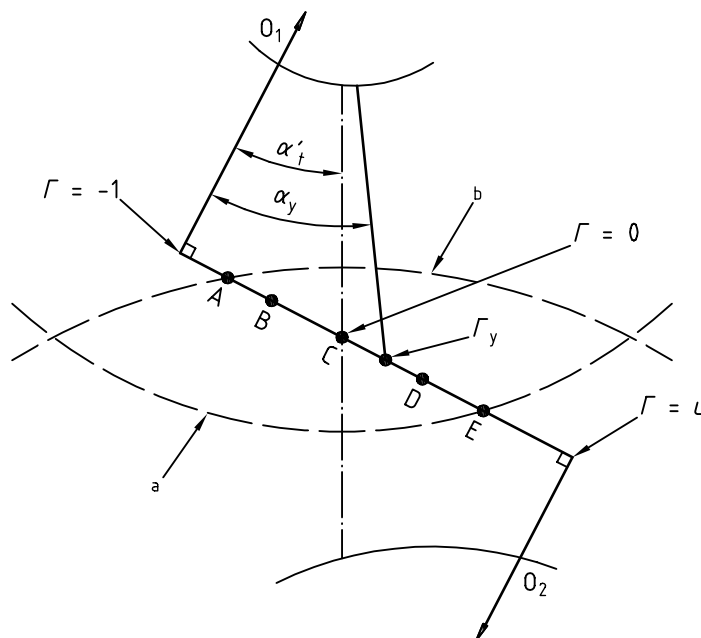
$\Phi_E = 0$, newly manufactured.

5.3 Thermal flash factor X_M

The thermal flash factor X_M accounts for the influence of the properties of pinion and gear materials on the flash temperature.

Calculation of the thermal flash factor for an arbitrary point (index y) on the line of action (see Figure 2):

$$X_M = \left[\frac{2}{\frac{1 - \nu_1^2}{E_1} + \frac{1 - \nu_2^2}{E_2}} \right]^{0,25} \cdot \frac{\sqrt{(1 + \Gamma)} + \sqrt{\left(1 - \frac{\Gamma}{u}\right)}}{B_{M1} \cdot \sqrt{(1 + \Gamma)} + B_{M2} \cdot \sqrt{\left(1 - \frac{\Gamma}{u}\right)}} \tag{9}$$



- a Tip circle 1
- b Tip circle 2

Figure 2 — Parameter Γ on the line of action

$$\Gamma_y = \frac{\tan \alpha_y}{\tan \alpha'_t} - 1 \quad (10)$$

If the materials of pinion and wheel are the same Equation (9) can be simplified to:

$$X_M = \frac{E^{0,25}}{(1-\nu^2)^{0,25} \cdot B_M} \quad (11)$$

In the above equations the thermal contact coefficient B_M is:

$$B_M = \sqrt{(\lambda_M \cdot c_v)} \quad (12)$$

For case hardened steels with the following typical characteristic values:

$$\lambda_M = 50 \text{ N/(s}\cdot\text{K)}, c_v = 3,8 \text{ N/(mm}^2\cdot\text{K)}, E = 206\,000 \text{ N/mm}^2 \text{ and } \nu = 0,3$$

follows

$$X_M = 50,0 \text{ K}\cdot\text{N}^{-0,75} \cdot \text{s}^{0,5} \cdot \text{m}^{-0,5} \cdot \text{mm}$$

For the characteristic values of other materials, see [7].

5.4 Pressure angle factor $X_{\alpha\beta}$

The pressure angle factor $X_{\alpha\beta}$ is used to account for the conversion of load and tangential speed from reference circle to pitch circle.

Method A: Factor $X_{\alpha\beta-A}$

$$X_{\alpha\beta-A} = 1,22 \cdot \frac{(\sin^{0,25} \alpha'_t \cdot \cos^{0,25} \alpha_n \cdot \cos^{0,25} \beta)}{(\cos^{0,5} \alpha'_t \cdot \cos^{0,5} \alpha_t)} \quad (13)$$

Table 2 shows the values for the pressure angle factor $X_{\alpha\beta}$ for a standard rack with pressure angle $\alpha_n = 20^\circ$, the typical range of standard working pressure angles α'_t and helix angles β .

Table 2 — Method B: Factor $X_{\alpha\beta-B}$

α'_t	$\beta = 0^\circ$	$\beta = 10^\circ$	$\beta = 20^\circ$	$\beta = 30^\circ$
19°	0,963	0,960	0,951	0,938
20°	0,978	0,975	0,966	0,952
21°	0,992	0,989	0,981	0,966
22°	1,007	1,004	0,995	0,981
23°	1,021	1,018	1,009	0,995
24°	1,035	1,032	1,023	1,008
25°	1,049	1,046	1,037	1,012

As an approximation, for gears with normal pressure angle $\alpha_n = 20^\circ$, the pressure angle factor can be approximated as follows:

$$X_{\alpha\beta-B} = 1$$

6 Calculation

6.1 Cylindrical gears

This part of ISO/TR 13989 contains equations which enable the assessment of the "probability of scuffing" (warm scuffing) of oil lubricated, involute spur and helical gears.

It is assumed that the total tangential load is equally distributed between the two helices of double helical gears. When, due to application of forces such as external axial forces, this is not the case, the influences of these are to be taken into account separately. The two helices are to be treated as parallel single helical gears. Influences affecting scuffing probability, for which quantitative assessments can be made, are included.

The equations are valid for gears with external or internal teeth which are conjugate to a basic rack as defined in ISO 53. For internal gears negative values have to be introduced for the determination of the geometry factor X_{BE} as presented in 6.1.10. They may also be considered as valid for similar gears of other basic rack form, of which the transverse contact ratio is $\varepsilon_{\alpha} \leq 2,5$.

6.1.1 Scuffing safety factor S_{intS}

As uncertainties and inaccuracies in the assumptions cannot be excluded, it is necessary to introduce a safety factor S_{intS} . It must be pointed out that the scuffing safety factor is temperature related and is not a factor by which gear torque may be multiplied to arrive at same values for the integral temperature number ϑ_{int} and the scuffing integral temperature number ϑ_{intS} .

$$S_{intS} = \frac{\vartheta_{intS}}{\vartheta_{int}} \geq S_{Smin} \quad (14)$$

Recommendation for choosing S_{Smin} :

$S_{Smin} < 1$	High scuffing risk
$1 \leq S_{Smin} \leq 2$	Critical range with moderate scuffing risk, influenced by the operating conditions of the actual gear. Influencing factors are e.g. the tooth flank roughness, run-in effects, the accurate knowledge of the load factors, the load capacity of lubricating oil, etc.
$S_{Smin} > 2$	Low scuffing risk

Given the relationship between the actual load and the integral temperature number, the corresponding load safety factor S_{SI} can be approximated by:

$$S_{SI} = \frac{w_{Btmax}}{w_{Bteff}} \approx \frac{\vartheta_{intS} - \vartheta_{oil}}{\vartheta_{int} - \vartheta_{oil}} \quad (15)$$

6.1.2 Permissible integral temperature ϑ_{intP}

$$\vartheta_{intP} = \frac{\vartheta_{intS}}{S_{Smin}} \quad (16)$$

The minimum required scuffing safety factor S_{Smin} is to be separately determined for each application.

6.1.3 Integral temperature ϑ_{int}

$$\vartheta_{int} = \vartheta_M + C_2 \cdot \vartheta_{flaint} \leq \vartheta_{intP} \quad (17)$$

where C_2 is the weighting factor derived from experiments. For spur and helical gears $C_2 = 1,5$.

$$\vartheta_{\text{flaint}} = \vartheta_{\text{flaE}} \cdot X_{\varepsilon} \quad (18)$$

6.1.4 Flash temperature at pinion tooth tip ϑ_{flaE}

$$\vartheta_{\text{flaE}} = \mu_{\text{mC}} \cdot X_{\text{M}} \cdot X_{\text{BE}} \cdot X_{\alpha\beta} \cdot \frac{(K_{\text{By}} \cdot w_{\text{Bt}})^{0,75} \cdot v^{0,5}}{|a|^{0,25}} \cdot \frac{X_{\text{E}}}{X_{\text{Q}} \cdot X_{\text{Ca}}} \quad (19)$$

6.1.5 Bulk temperature ϑ_{M}

The bulk temperature is the temperature of the tooth surfaces immediately before they come into contact.

The bulk temperature is established by the thermal balance of the gear unit. There are several sources of heat in a gear unit of which the most important are tooth and bearing friction. Other sources of heat such as seals and oil flow contribute to some extent. At pitch line velocities in excess of 80 m/s, heat from the churning of oil in the mesh and windage losses may become significant and should be taken into consideration (see Method A). The heat is transferred to the environment via the housing walls by conduction, convection and radiation and for spray lubrication conditions through the oil into an external heat exchanger.

Values obtained using the different calculation methods described below are to be distinguished by the subscripts A, B, C.

6.1.5.1 Method A $\vartheta_{\text{M-A}}$

The bulk temperature as a mean value or as temperature distribution over the facewidth can be measured experimentally or be determined by a theoretical analysis based on known power loss and heat transfer data, i.e. by using thermal network methods.

6.1.5.2 Method B $\vartheta_{\text{M-B}}$

This method is not used for the integral temperature method (see the flash temperature method given in ISO/TR 13989-1).

6.1.5.3 Method C $\vartheta_{\text{M-C}}$

An approximate value for the bulk temperature consists of the sum of the oil temperature and a part of a mean value derived from the flash temperature over the path of contact according to method C.

$$\vartheta_{\text{M-C}} = \vartheta_{\text{oil}} + C_1 \cdot X_{\text{mp}} \cdot \vartheta_{\text{flaint}} \cdot X_{\text{S}} \quad (20)$$

where

$X_{\text{S}} = 1,2$ for spray lubrication;

$X_{\text{S}} = 1,0$ for dip lubrication;

$X_{\text{S}} = 0,2$ for gears submerged in oil;

C_1 is the constant accounting for heat transfer conditions, from test results $C_1 = 0,7$;

$$X_{\text{mp}} = \frac{1 + n_{\text{p}}}{2} \quad (21)$$

where n_{p} is the number of meshing gears.

6.1.6 Mean coefficient of friction μ_{mC}

See 5.1.

6.1.7 Run-in factor X_E

See 5.2.

6.1.8 Thermal flash factor X_M

See 5.3.

6.1.9 Pressure angle factor $X_{\alpha\beta}$

See 5.4.

6.1.10 Geometry factor at tip of pinion X_{BE}

The geometry factor X_{BE} takes into account Hertzian stress and sliding velocity at the pinion tooth tip. X_{BE} is a function of the gear ratio u and the radius of curvature ρ_E at the pinion tooth tip E.

For internal gears the following parameters have to be introduced as negative values:

number of teeth z_2 , gear ratio u , centre distance a and all diameters

$$X_{BE} = 0,51 \cdot \sqrt{\frac{|z_2|}{z_2}} \cdot (u + 1) \cdot \frac{\sqrt{\rho_{E1}} - \sqrt{\frac{\rho_{E2}}{u}}}{(\rho_{E1} \cdot |\rho_{E2}|)^{0,25}} \quad (22)$$

$$\rho_{E1} = 0,5 \cdot \sqrt{d_{a1}^2 - d_{b1}^2} \quad (23)$$

$$\rho_{E2} = a \cdot \sin \alpha'_t - \rho_{E1} \quad (24)$$

6.1.11 Approach factor X_Q

The approach factor X_Q takes into account impact loads at the ingoing mesh (at tooth tip of driven gear) in areas of high sliding. It is represented by a function of the quotient of the approach contact ratio ε_f over the recess contact ratio ε_a , see Figure 3.

$$X_Q = 1,00 \quad \text{for } \frac{\varepsilon_f}{\varepsilon_a} \leq 1,5 \quad (25)$$

$$X_Q = 1,40 - \frac{4}{15} \cdot \frac{\varepsilon_f}{\varepsilon_a} \quad \text{for } 1,5 < \frac{\varepsilon_f}{\varepsilon_a} < 3 \quad (26)$$

$$X_Q = 0,60 \quad \text{for } 3 \leq \frac{\varepsilon_f}{\varepsilon_a} \quad (27)$$

$$\left. \begin{array}{l} \varepsilon_f = \varepsilon_2 \\ \varepsilon_a = \varepsilon_1 \end{array} \right\} \text{ when the pinion drives the wheel} \quad (28)$$

$$\left. \begin{array}{l} \varepsilon_f = \varepsilon_1 \\ \varepsilon_a = \varepsilon_2 \end{array} \right\} \text{ when the pinion is driven by the wheel} \quad (29)$$

$$\varepsilon_1 = \frac{z_1}{2\pi} \cdot \left[\sqrt{\left(\frac{d_{a1}}{d_{b1}}\right)^2 - 1} - \tan \alpha'_t \right] \quad (30)$$

$$\varepsilon_2 = \frac{|z_2|}{2\pi} \cdot \left[\sqrt{\left(\frac{d_{a2}}{d_{b2}}\right)^2 - 1} - \tan \alpha'_t \right] \quad (31)$$

When tooth tips are chamfered or rounded, the tip diameter d_a has to be substituted by the effective tip diameter d_{Na} at which the recess is starting.

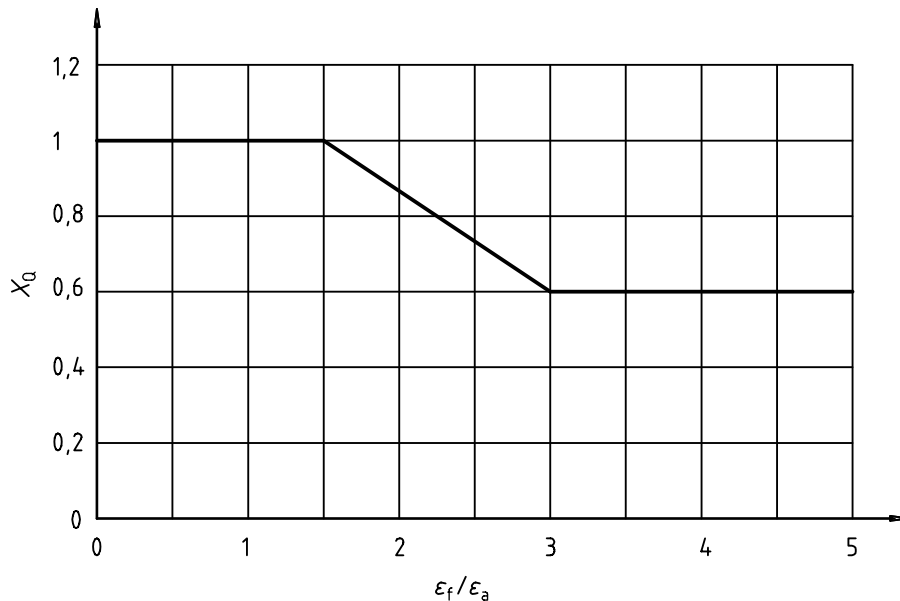


Figure 3 — Approach factor X_Q

6.1.12 Tip relief factor X_{Ca}

Elastic deformations of loaded teeth may cause high impact loads at tooth tips in areas of relatively high sliding. The tip relief factor X_{Ca} takes account of the influences of profile modifications on such loads. X_{Ca} is a relative tip relief factor which depends on the actual amount of tip relief C_a related to the effective tip relief due to elastic deformation C_{eff} , see Figure 4.

The curves in Figure 4 can be approximated by the equation

$$X_{Ca} = 1 + \left[0,06 + 0,18 \left(\frac{C_a}{C_{eff}} \right) \right] \cdot \varepsilon_{max} + \left[0,02 + 0,69 \left(\frac{C_a}{C_{eff}} \right) \right] \cdot \varepsilon_{max}^2 \quad (32)$$

where ε_{max} is the maximum value, ε_1 or ε_2 .

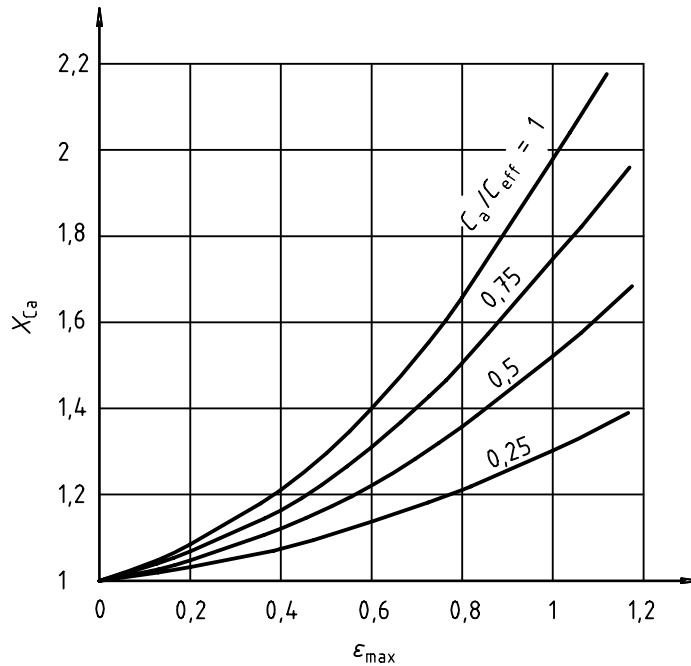


Figure 4 — Tip relief factor X_{Ca} due to experimental data [8, 9]

The nominal amount of tip relief C_a to be introduced into Equation (32) depends on the actual values of tip relief C_{a1} , C_{a2} , the effective tip relief C_{eff} , the ratio of addendum contact ratios and the direction of power flow.

When the pinion drives the wheel and $\epsilon_1 > 1,5 \epsilon_2$ or the pinion is driven by the wheel and $\epsilon_1 > (2/3)\epsilon_2$,

$$C_a = C_{a1} \quad \text{for} \quad C_{a1} \leq C_{eff} \tag{33}$$

$$C_a = C_{eff} \quad \text{for} \quad C_{a1} > C_{eff} \tag{34}$$

when the pinion drives the wheel and $\epsilon_1 \leq 1,5 \epsilon_2$ or the pinion is driven by the wheel and $\epsilon_1 < (2/3)\epsilon_2$,

$$C_a = C_{a2} \quad \text{for} \quad C_{a2} \leq C_{eff} \tag{35}$$

$$C_a = C_{eff} \quad \text{for} \quad C_{a2} > C_{eff} \tag{36}$$

where C_{eff} is the effective tip relief, that amount of tip relief which compensates for the elastic deformation of the teeth in single pair contact.

$$C_{eff} = \frac{K_A \cdot F_t}{b \cdot c'} \quad \text{for spur gears} \tag{37}$$

$$C_{eff} = \frac{K_A \cdot F_t}{b \cdot c_\gamma} \quad \text{for helical gears} \tag{38}$$

where b is the facewidth. If the facewidth of the pinion is different from that of the wheel, the smaller is determining.

Tip relief as described above applies to gears of ISO accuracy grade 6 or better, in accordance with ISO 1328-1. For less accurate gears, X_{Ca} is to be set equal to 1; see also ISO 6336-1.

6.1.13 Contact ratio factor: X_ϵ

The contact ratio factor X_ϵ converts the flash temperature value at the pinion tooth tip when load sharing is neglected, to a mean value of the flash temperature over the path of contact. The contact ratio factor can be expressed in terms of addendum contact ratios ϵ_1 and ϵ_2 , and their sum ϵ_α . The equations for X_ϵ are based on an

assumed linearity of the flash temperature over the path of contact. Possible errors due to this approach will be unlikely to exceed 5 % and will always be on the safe side.

For $\varepsilon_\alpha < 1$, $\varepsilon_1 < 1$, $\varepsilon_2 < 1$:

$$X_\varepsilon = \frac{1}{2 \cdot \varepsilon_\alpha \cdot \varepsilon_1} \cdot (\varepsilon_1^2 + \varepsilon_2^2) \quad (39)$$

For $1 \leq \varepsilon_\alpha < 2$, $\varepsilon_1 < 1$, $\varepsilon_2 < 1$ (see Figure 5):

$$X_\varepsilon = \frac{1}{2 \cdot \varepsilon_\alpha \cdot \varepsilon_1} \cdot \left[0,70 \cdot (\varepsilon_1^2 + \varepsilon_2^2) - 0,22 \cdot \varepsilon_\alpha + 0,52 - 0,60 \cdot \varepsilon_1 \cdot \varepsilon_2 \right] \quad (40)$$

For $1 \leq \varepsilon_\alpha < 2$, $\varepsilon_1 \geq 1$, $\varepsilon_2 < 1$:

$$X_\varepsilon = \frac{1}{2 \cdot \varepsilon_\alpha \cdot \varepsilon_1} \cdot (0,18 \cdot \varepsilon_1^2 + 0,70 \cdot \varepsilon_2^2 + 0,82 \cdot \varepsilon_1 - 0,52 \cdot \varepsilon_2 - 0,30 \cdot \varepsilon_1 \cdot \varepsilon_2) \quad (41)$$

For $1 \leq \varepsilon_\alpha < 2$, $\varepsilon_1 < 1$, $\varepsilon_2 \geq 1$:

$$X_\varepsilon = \frac{1}{2 \cdot \varepsilon_\alpha \cdot \varepsilon_1} \cdot (0,70 \cdot \varepsilon_1^2 + 0,18 \cdot \varepsilon_2^2 - 0,52 \cdot \varepsilon_1 + 0,82 \cdot \varepsilon_2 - 0,30 \cdot \varepsilon_1 \cdot \varepsilon_2) \quad (42)$$

For $2 \leq \varepsilon_\alpha < 3$, $\varepsilon_1 \geq \varepsilon_2$ (see Figure 6):

$$X_\varepsilon = \frac{1}{2 \cdot \varepsilon_\alpha \cdot \varepsilon_1} \cdot (0,44 \cdot \varepsilon_1^2 + 0,59 \cdot \varepsilon_2^2 + 0,30 \cdot \varepsilon_1 - 0,30 \cdot \varepsilon_2 - 0,15 \cdot \varepsilon_1 \cdot \varepsilon_2) \quad (43)$$

For $2 \leq \varepsilon_\alpha < 3$, $\varepsilon_1 < \varepsilon_2$ (see Figure 6):

$$X_\varepsilon = \frac{1}{2 \cdot \varepsilon_\alpha \cdot \varepsilon_1} \cdot (0,59 \cdot \varepsilon_1^2 + 0,44 \cdot \varepsilon_2^2 - 0,30 \cdot \varepsilon_1 + 0,30 \cdot \varepsilon_2 - 0,15 \cdot \varepsilon_1 \cdot \varepsilon_2) \quad (44)$$

$$\varepsilon_\alpha = \varepsilon_1 + \varepsilon_2 \quad (45)$$

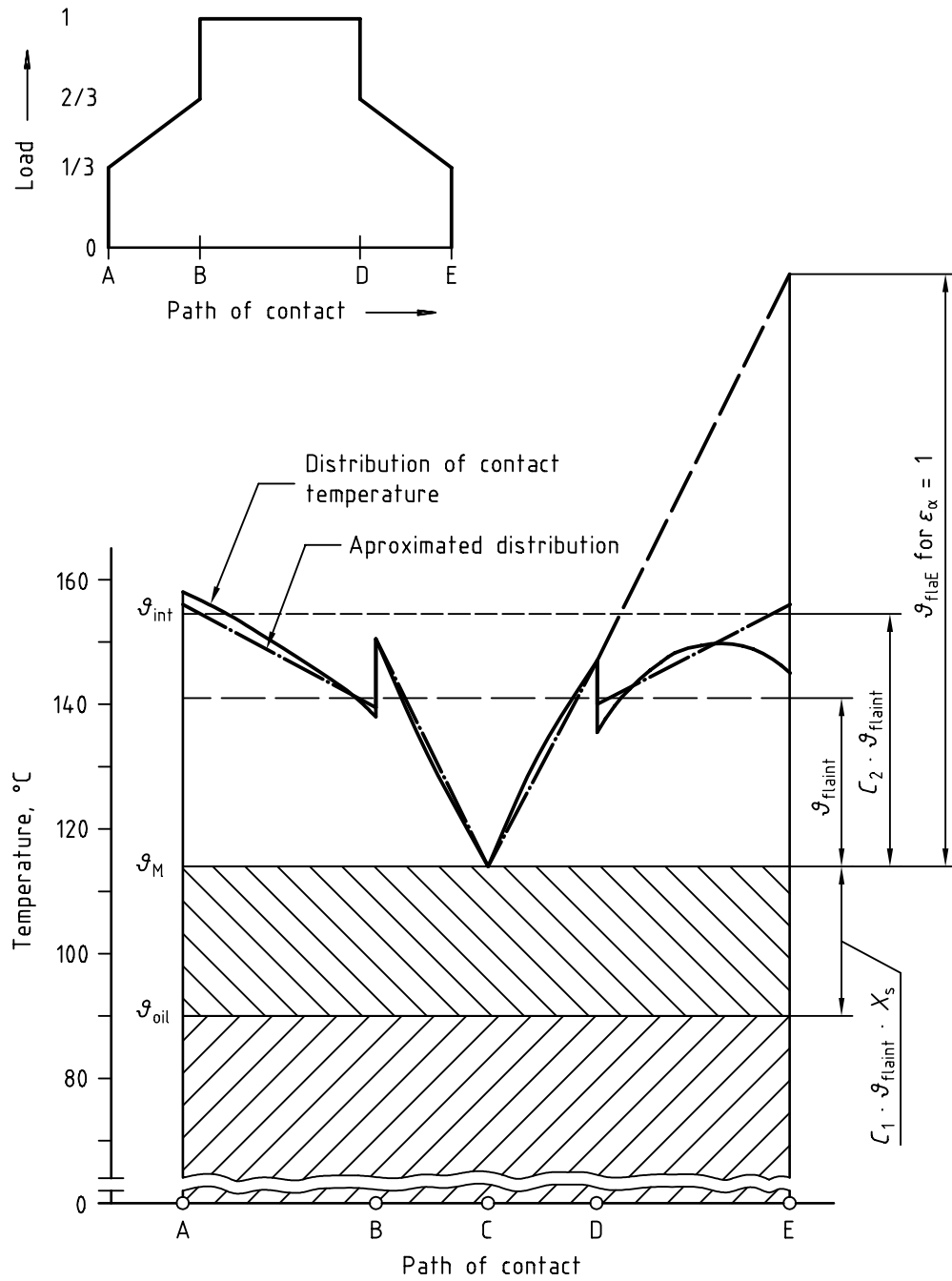
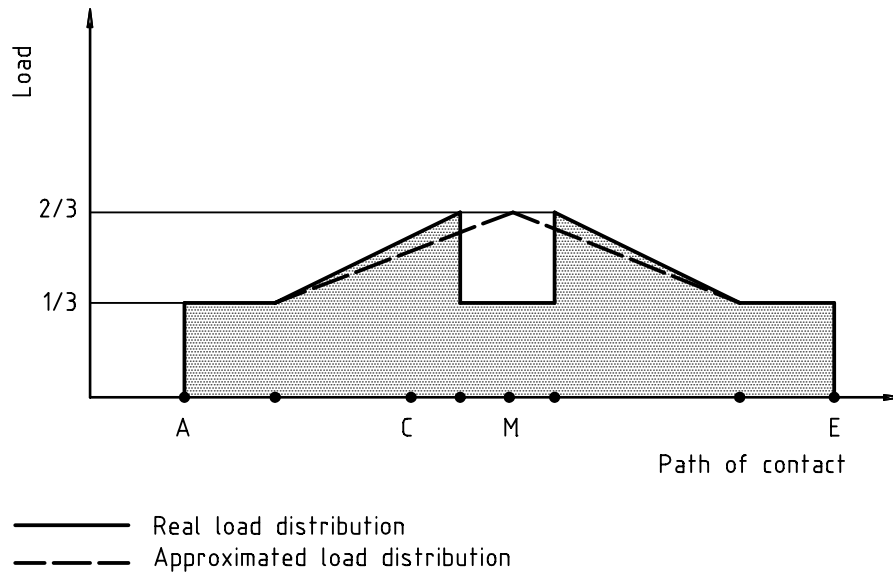
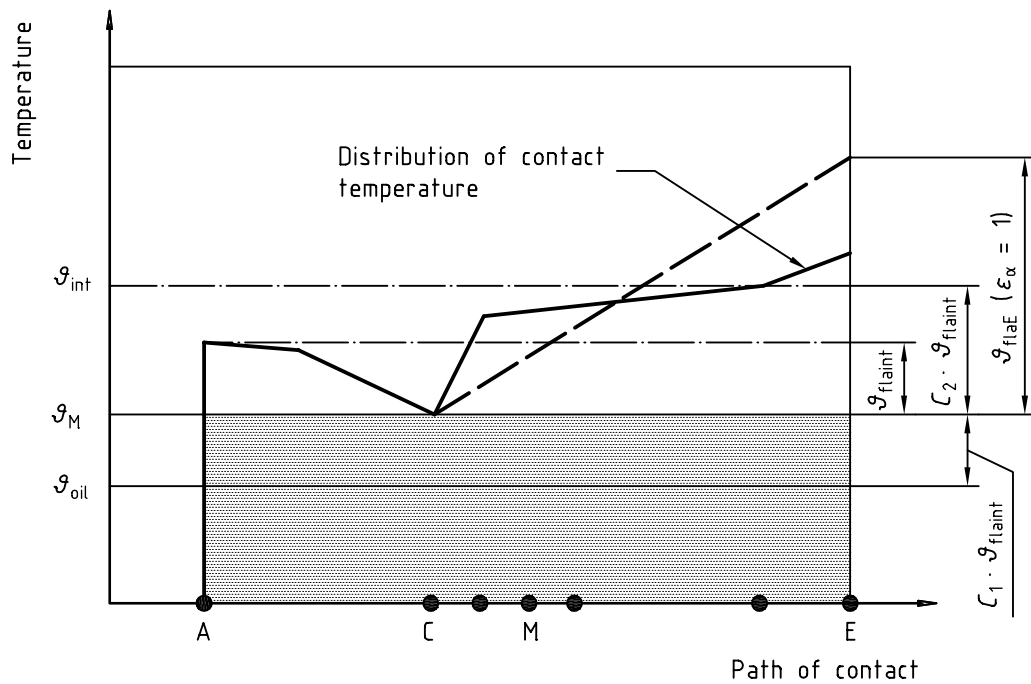


Figure 5 — Load and temperature distribution for $1,0 \leq \epsilon_{\alpha} < 2,0$



a) Load distribution along the path of contact



b) Temperature distribution along the path of contact

Figure 6 — Load and temperature distribution for $2,0 \leq \varepsilon_\alpha < 3,0$

6.2 Bevel gears

This part of ISO/TR 13989 follows the integral temperature method as described in 6.1.

For the calculation, the bevel gears are approximated by equivalent cylindrical gears at the mean diameter d_m of the bevel gear set (see ISO 10300-1 for the calculation of the virtual cylindrical gear). For this reason, the structure of the calculation methods specified in this part of ISO/TR 13989 corresponds to that of cylindrical gears.

Scuffing is calculated according to 6.1 for the virtual cylindrical gear substituting the bevel gear at the mean diameter in the transverse section.

6.2.1 Scuffing safety factor S_{intS}

See 6.1.1.

6.2.2 Permissible integral temperature \mathcal{G}_{IntP}

See 6.1.2.

6.2.3 Integral temperature \mathcal{G}_{Int}

See 6.1.3.

$C_2 = 1,5$ for virtual cylindrical gear

6.2.4 Flash temperature at pinion tooth tip \mathcal{G}_{flaE}

See 6.1.4, with the following substitutions:

- in equation (19): a_v instead of a
 v_{mt} instead of v
- in equation (4): F_{mt} instead of F_t
 b_{eB} instead of b

The effective face width b_{eB} takes account of the crowning of bevel gears.

$$b_{eB} = 0,85b_2 \tag{46}$$

where b_2 is the common tooth width of pinion and wheel.

The factors $K_A, K_v, K_{B\beta} = K_{H\beta}$ and $K_{B\alpha} = K_{H\alpha}$ shall be determined in accordance with ISO 10300-1.

$$K_{B\gamma} = 1$$

6.2.5 Bulk temperature \mathcal{G}_M

See 6.1.5.

6.2.6 Mean coefficient of friction μ_{mC}

See 5.1, with the following substitutions:

- in equation (4): F_{mt} instead of F_t
 b_{eB} instead of b

For the conditions of usual bevel gear design $\alpha_t' = \alpha_{vt}$, i.e. $x_1 = -x_2$:

$$v_{\Sigma C} = 2 \cdot v_{mt} \cdot \sin \alpha_{vt} \tag{47}$$

$$K_{B\gamma} = 1$$

6.2.7 Run-in factor X_E

See 5.2.

6.2.8 Thermal flash factor X_M

See 5.3.

6.2.9 Pressure angle factor $X_{\alpha\beta}$ **6.2.9.1 Method A: Factor $X_{\alpha\beta-A}$**

For the conditions of usual bevel gear design $\alpha_t' = \alpha_{vt}$, i.e. $x_1 = -x_2$:

$$X_{\alpha\beta-A} = 1,22 \cdot \frac{\sin^{0,25} \alpha_n}{\cos^{0,75} \alpha_{vt}} \quad (48)$$

6.2.9.2 Method B: Factor $X_{\alpha\beta-B}$

See 5.4.

6.2.10 Geometry factor at tip of pinion X_{BE}

See 6.1.10, with the following substitutions:

- in equation (22): u_v instead of u
- in equation (23): d_{va1} instead of d_{a1}
 d_{vb1} instead of d_{b1}
- in equation (24): α_{vt} instead of α_t'

6.2.11 Approach factor X_Q

See 6.1.11, with the following substitutions:

- in equations (28) to (31): ε_{v1} instead of ε_1
 ε_{v2} instead of ε_2
- in equations (30) and (31): $d_{va1,2}$ instead of $d_{a1,2}$
 $d_{vb1,2}$ instead of $d_{b1,2}$
 α_{vt} instead of α_t'
 $z_{v1,2}$ instead of $z_{1,2}$

6.2.12 Tip relief factor X_{Ca}

See 6.1.12, with the following substitution:

- in equation (32): ε_{vmax} instead of ε_{max}
 ε_{vmax} maximum value ε_{v1} or ε_{v2}

It is assumed that tip and root relief are chosen as optimum values for the operation conditions (full-load contact pattern spreads just to tip without concentration). Then the following approximation applies:

$$C_a = C_{\text{eff}} \quad \text{and} \quad \frac{C_a}{C_{\text{eff}}} = 1 \quad (49)$$

6.2.13 Contact ratio factor X_ε

See 6.1.13, with the following substitutions in Eqs. (39) to (45) and its conditions of validity:

$\varepsilon_{V\alpha}$ instead of ε_α

ε_{V1} instead of ε_1

ε_{V2} instead of ε_2

6.3 Hypoid gears

This calculation method of the scuffing resistance of hypoid gears follows the integral temperature criterion of cylindrical gears according to 6.1.

For the calculation of the scuffing resistance, the hypoid gears are approximated by equivalent crossed axes helical gears with the same sliding conditions as the actual hypoid gears (see 6.3.11 for the virtual crossed axes helical gear pair).

6.3.1 Scuffing safety factor S_{intS}

See 6.1.1.

6.3.2 Permissible integral temperature ϑ_{intP}

See 6.1.2.

6.3.3 Integral temperature ϑ_{int}

See 6.1.3, with the following substitutions:

— in equation (17): C_{2H} instead of C_2 ($C_{2H} = 1,8$ according to test results)

$\vartheta_{\text{flainth}}$ instead of $\vartheta_{\text{flaint}}$

$$\vartheta_{\text{flainth}} = 110 \cdot \sqrt{F_n \cdot K_A \cdot K_{B\beta} \cdot v_{t1} \cdot \mu_{mC}} \cdot \frac{X_E \cdot X_G \cdot X_\varepsilon}{X_Q \cdot X_{CA}} \quad (50)$$

$$F_n = \frac{2000 \cdot T_1}{\cos \alpha_{mn} \cdot \cos \beta_{m1} \cdot d_{m1}} \quad (51)$$

$$K_{B\beta} = 1,5 \cdot K_{B\beta\text{be}} \quad (52)$$

$$K_{B\beta\text{be}} = K_{H\beta\text{be}} \quad (\text{see ISO 10300-1})$$

6.3.4 Bulk temperature ϑ_M

See 6.1.5.

6.3.5 Mean coefficient of friction μ_{mC}

See 5.1, with the following substitutions:

- in equation (1): ρ_{Cn} instead of ρ_{redC}
- in equation (4): $b_{eB}/\cos\beta_{b2}$ instead of b
 F_n instead of F_t

b_{eB} : see equation (46).

$$K_{B\gamma} = 1$$

$$K_{B\gamma} \cdot K_{B\alpha} = 2,0 \text{ (approximation only for the calculation of } \mu_{mC}\text{)} \quad (53)$$

X_R : see equation (7), with ρ_{Cn} instead of ρ_{redC} .

6.3.6 Run-in factor X_E

See 5.2, with the following substitution in equation (8):

- ρ_{Cn} instead of ρ_{redC}

6.3.7 Geometry factor X_G

The geometry factor X_G accounts for the mean Hertzian stress and the mean contact length along the path of contact. As an approximation it can be determined by using the values at the pitch point (ρ_{Cn} , L).

$$X_G = \frac{\left(\frac{\sin \Sigma}{\cos \beta_{s2}} \right) \cdot \sqrt{\frac{1}{\rho_{Cn}}}}{\sqrt{L \cdot \sin \beta_{s1}} + \sqrt{L \cdot \cos \beta_{s1} \cdot \tan \beta_{s2}}} \quad (54)$$

$$L = \frac{2}{3} \cdot \xi^2 \cdot \eta \quad (55)$$

For ξ and η see Figure 7 or equations (57) to (60) according to [10].

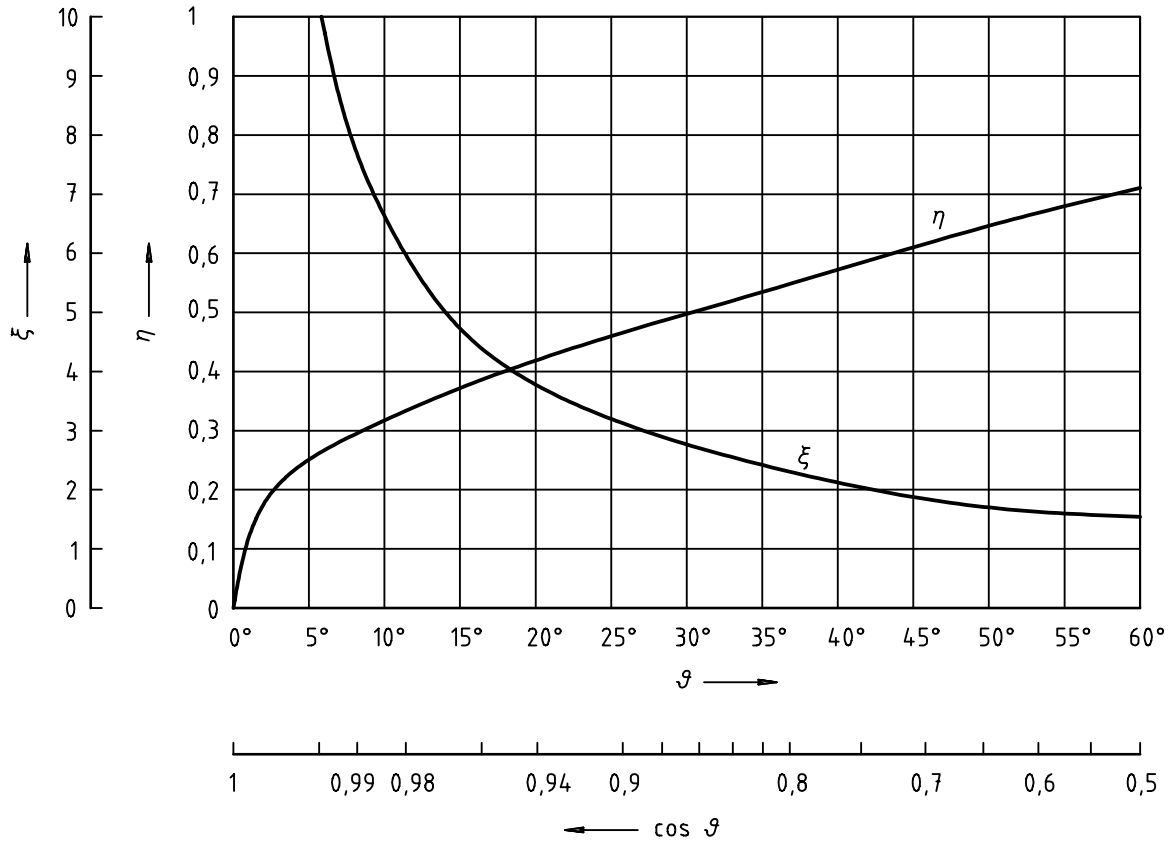


Figure 7 — The auxiliary coefficients ξ and η as a function of $\cos \vartheta$

$$\cos \vartheta = \rho_{Cn} \sqrt{\frac{1}{\rho_{n1}^2} + \frac{1}{\rho_{n2}^2} + \frac{2 \cdot \cos 2\vartheta}{\rho_{n1} \cdot \rho_{n2}}} \tag{56}$$

for $0 \leq \cos \vartheta < 0,949$:

$$\ln \xi = \frac{\ln(1 - \cos \vartheta)}{-1,53 + 0,333 \cdot \ln(1 - \cos \vartheta) + 0,0467 \cdot [\ln(1 - \cos \vartheta)]^2} \tag{57}$$

$$\ln \eta = \frac{\ln(1 - \cos \vartheta)}{1,525 - 0,86 \cdot \ln(1 - \cos \vartheta) - 0,0993 \cdot [\ln(1 - \cos \vartheta)]^2} \tag{58}$$

for $0,949 \leq \cos \vartheta < 1$:

$$\ln \xi = \sqrt{-0,4567 - 0,4446 \cdot \ln(1 - \cos \vartheta) + 0,1238 \cdot [\ln(1 - \cos \vartheta)]^2} \tag{59}$$

$$\ln \eta = -0,333 + 0,2037 \cdot \ln(1 - \cos \vartheta) + 0,0012 \cdot [\ln(1 - \cos \vartheta)]^2 \tag{60}$$

6.3.8 Approach factor X_Q

See 6.1.11, with the following substitutions:

— in equations (28) to (31): ε_{n1} instead of ε_1

ε_{n2} instead of ε_2

6.3.9 Tip relief factor X_{Ca}

See 6.1.12, with the following substitution

— in equation (32): $\varepsilon_{n\max}$ instead of ε_{\max}

$\varepsilon_{n\max}$ maximum value of ε_{n1} or ε_{n2}

For adequate tip and root relief:

$$C_a/C_{\text{eff}} = 1, \text{ see 6.2.12}$$

6.3.10 Contact ratio factor X_ε

$$X_\varepsilon = \frac{1}{\sqrt{\varepsilon_n}} \cdot \left[1 + 0,5 \cdot g^* \cdot \left(\frac{v_{g\gamma 1}}{v_{gs} - 1} \right) \right] \quad (61)$$

$$g^* = \frac{g_{an1}^2 + g_{an2}^2}{g_{an1}^2 + g_{an1} \cdot g_{an2}} \quad (62)$$

For gear pairs with about the same length of recess paths ($g_{an1} \approx g_{an2}$) the sliding factor g^* is close to unity.

6.3.11 Calculation of virtual crossed axes helical gears

This part contains geometrical relationships to convert a hypoid gear pair to a crossed axes helical gear pair. The conditions at mid-facewidth of hypoid gears are taken as basis for conversion (see Figure 8).

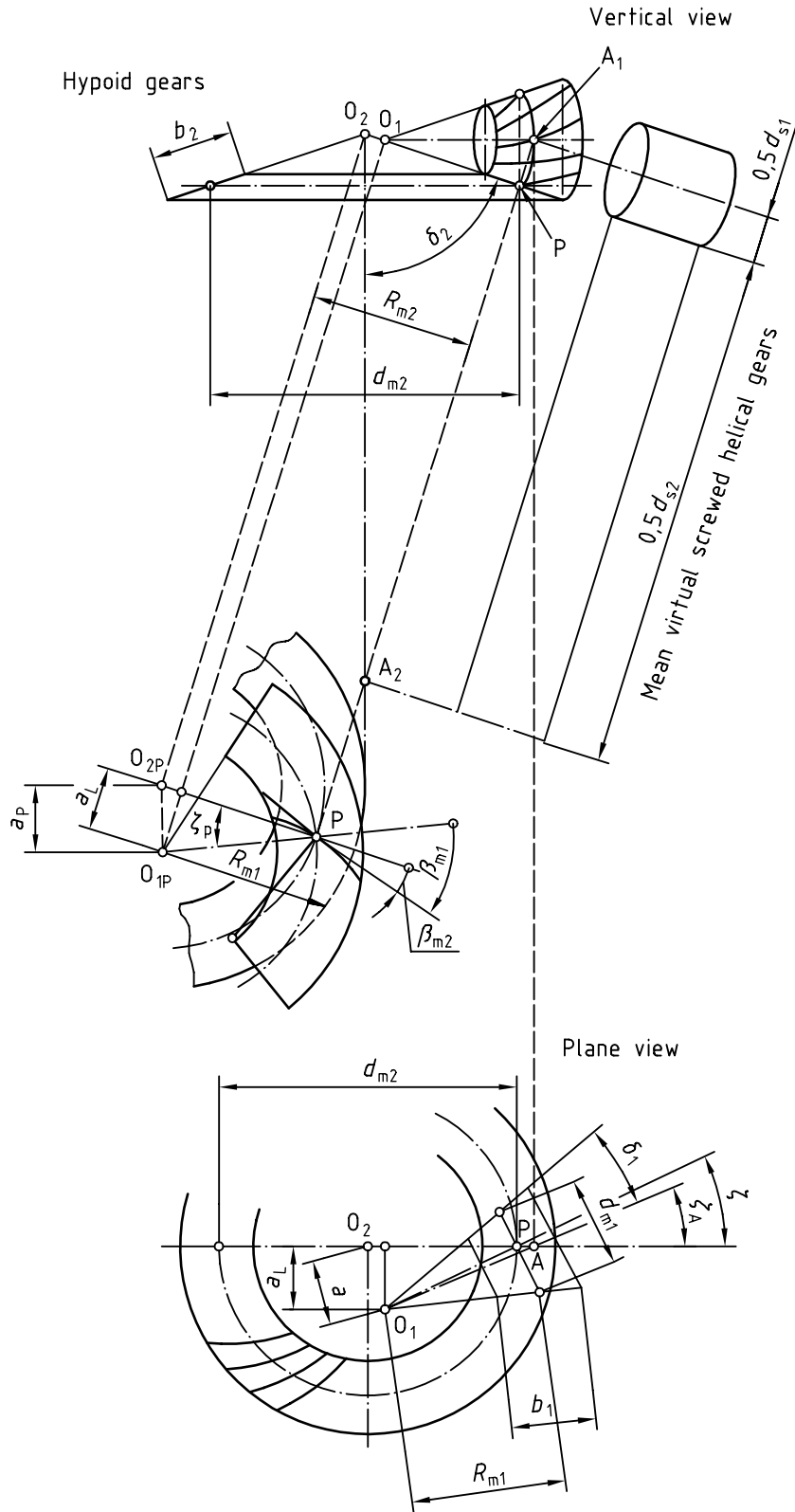


Figure 8 — For the calculation of virtual crossed axes helical gears

Data of the virtual crossed axes helical gear:

Helix angle

$$\beta_{s1,2} = \beta_{m1,2}$$

(63)

Normal pressure angle

$$\alpha_{sn} = \alpha_{mn} \quad (64)$$

Crossing angle of crossed axes helical gear

$$\Sigma = \beta_{m1} - \beta_{m2} \quad (65)$$

Transverse pressure angle $\alpha_{st1,2}$

$$\tan \alpha_{st1,2} = \frac{\tan \alpha_{sn}}{\cos \beta_{s1,2}} \quad (66)$$

Base helix angle $\beta_{b1,2}$

$$\sin \beta_{b1,2} = \frac{\sin \beta_{s1,2}}{\cos \alpha_{sn}} \quad (67)$$

Reference circle

$$d_{s1,2} = \frac{d_{m1,2}}{\cos \delta_{1,2}} \quad (68)$$

Tip diameter

$$d_{a1,2} = d_{s1,2} + 2h_{am1,2} \quad (69)$$

Base circle

$$d_{b1,2} = d_{s1,2} \cdot \cos \alpha_{t1,2} \quad (70)$$

Axle angle of crossed axes helical gear

$$\tan \beta_{b1,2} = \tan \beta_{m1,2} \cdot \sin \alpha_{mn} \quad (71)$$

$$\varphi = \beta_{b1} + \beta_{b2} \quad (72)$$

Module

$$m_{sn} = m_{mn} \quad (73)$$

Normal base pitch

$$p_{en} = m_{sn} \cdot \pi \cdot \cos \alpha_{sn} \quad (74)$$

Radii of curvature in normal section

$$\rho_{n1,2} = 0,5 \cdot d_{s1,2} \cdot \frac{\sin^2 \alpha_{t1,2}}{\sin \alpha_{sn}} \quad (75)$$

$$\rho_{Cn} = \frac{\rho_{n1} \cdot \rho_{n2}}{\rho_{n1} + \rho_{n2}} \quad (76)$$

Tangential velocities

$$v_{t1} = \frac{\pi \cdot n_1 \cdot d_{m1}}{60\,000} \quad (77)$$

$$v_{t2} = v_{t1} \cdot \frac{\cos\beta_{s1}}{\cos\beta_{s2}} \quad (78)$$

Sum of the tangential speeds at pitch point $v_{\Sigma C}$ (β_{s1}, β_{s2} positive)

$$v_{\Sigma s} = v_{t1} \left(\sin\beta_{s1} + \sin\beta_{s2} \cdot \frac{\cos\beta_{s1}}{\cos\beta_{s2}} \right) \quad (79)$$

$$v_{\Sigma h} = 2v_{t1} \cos\beta_{s1} \sin\alpha_{sn} \quad (80)$$

$$v_{\Sigma C} = \sqrt{v_{\Sigma s}^2 + v_{\Sigma h}^2} \quad (81)$$

Sliding velocity at pitch point

$$v_{gs} = v_{t1} \frac{\sin\Sigma}{\cos\beta_{s2}} \quad (82)$$

Maximum sliding velocity at tip of pinion $v_{g\gamma 1}$

$$v_{g\gamma 1} = \sqrt{v_{g\alpha 1}^2 + v_{g\beta 1}^2} \quad (83)$$

$$v_{g1} = 2 \cdot v_{t1} \cdot g_{an1} \cdot \frac{\cos\beta_{b1}}{d_{s1}} \quad (84)$$

$$v_{g2} = 2 \cdot v_{t2} \cdot g_{fn2} \cdot \frac{\cos\beta_{b2}}{d_{s2}} \quad (85)$$

$$\gamma_{1,2} \text{ from } \tan\gamma_{1,2} = \sin\alpha_{sn} \cdot \tan\beta_{s1,2} \quad (86)$$

$$v_{g\alpha 1} = v_{g1} \cdot \cos\gamma_1 + v_{g2} \cdot \cos\gamma_2 \quad (87)$$

$$v_{g\beta 1} = v_{gs} + v_{g1} \cdot \sin\gamma_1 - v_{g2} \cdot \sin\gamma_2 \quad (88)$$

Path of contact

$$\overline{AE} = g_{an1} + g_{an2} \quad (89)$$

$$g_{an1} = \frac{g_{at1}}{\cos\beta_{b1}} = \frac{0,5 \left(\sqrt{d_{a1}^2 - d_{b1}^2} - \sqrt{d_{s1}^2 - d_{b1}^2} \right)}{\cos\beta_{b1}} = \overline{SE} = g_{fn2} \quad (90)$$

$$g_{an2} = \frac{0,5 \left(\sqrt{d_{a2}^2 - d_{b2}^2} - \sqrt{d_{s2}^2 - d_{b2}^2} \right)}{\cos\beta_{b2}} = \overline{SA} = g_{fn1} \quad (91)$$

Contact ratio in normal section

$$\varepsilon_n = \frac{\overline{AE}}{p_{en}} \quad (92)$$

$$\varepsilon_{n1,2} = \frac{g_{an1,2}}{p_{en}} \quad (93)$$

6.4 Scuffing integral temperature

The scuffing integral temperature is the limiting value of the temperature at which scuffing occurs. It can be calculated on the basis of test results.

This method is valid for all types of oils (pure mineral oils, EP-oils, synthetic oils) for which the scuffing load capacity has been determined in a test gear (suitable tests are for example the FZG-test A/8,3/90, the FZG L-42 test, the Ryder gear oil test or the IAE gear oil test), or by an actual case of damage.

The scuffing temperature must be corrected when material and heat treatment respectively of the test gear are not identical with that of the actual gear as the limiting temperature is a function of the material-oil system.

6.4.1 Scuffing integral temperature ϑ_{IntS}

According to the integral temperature postulate, gears are likely to scuff when the mean flank temperature exceeds a value termed the scuffing integral temperature number. This number is assumed to be characteristic for the lubricant and gear-material combination of a gear pair and is to be determined by testing a similar lubricant and gear-material combination.

A scuffing integral temperature number can be derived from the results of any gear oil scuffing test by entering the test data into the equations in 6.1, 6.2, 6.3. Thus scuffing integral temperature numbers for any oil: straight mineral, EP or synthetic, can be evaluated.

6.4.1.1 Calculation of the scuffing integral temperature

The approximate scuffing integral temperature number of heat- or surface-treated gear steels in combination with a mineral oil, can be derived from that of a combination of gear steels with other heat- or surface-treatments and the same lubricant.

$$\vartheta_{\text{IntS}} = \vartheta_{\text{MT}} + X_{\text{WreIT}} \cdot C_2 \cdot \vartheta_{\text{flaintT}} \quad (94)$$

where $C_2 = 1,5$; derived from experiments.

6.4.1.2 Determination of ϑ_{MT} , $\vartheta_{\text{flaintT}}$ from test results

Figure 9 shows the diagram for mineral oils in case that the scuffing load capacity is determined in an FZG-test A/8,3/90 in accordance with DIN 51354 [2], in a Ryder [3] or an FZG-Ryder test [4] and in an FZG L-42 test [5].

For computer calculations the diagrams in Figures 9 to 11 can be approximated by the following equations:

a) For the FZG test A/8,3/90:

$$\vartheta_{\text{MT}} = 80 + 0,23 \cdot T_{1\text{T}} \cdot X_{\text{L}} \quad (95)$$

$$\vartheta_{\text{flaintT}} = 0,2 \cdot T_{1\text{T}} \cdot \left(\frac{100}{v_{40}} \right)^{0,02} \cdot X_{\text{L}} \quad (96)$$

$$T_{1\text{T}} = 3,726 \cdot (\text{FZG load stage})^2 \quad (97)$$

b) For the Ryder and the FZG-Ryder test R/46,5/74:

$$\vartheta_{\text{MT}} = 90 + 0,0125 \left(\frac{F_{\text{bt}}}{b} \right)_{\text{T}} \cdot X_{\text{L}} \quad (98)$$

$$\vartheta_{\text{flaintT}} = 0,015 \left(\frac{F_{bt}}{b} \right)_T \cdot \left(\frac{100}{v_{40}} \right)^{0,03} \cdot X_L \tag{99}$$

with F_{bt}/b in lb/in.

c) For the FZG L-42 test 141/19,5/110:

$$\vartheta_{\text{MT}} = 110 + 0,02 \cdot T_{1T} \cdot X_L \tag{100}$$

$$\vartheta_{\text{flaintT}} = 0,48 T_{1T} \cdot \left(\frac{100}{v_{40}} \right)^{0,02} \cdot X_L \tag{101}$$

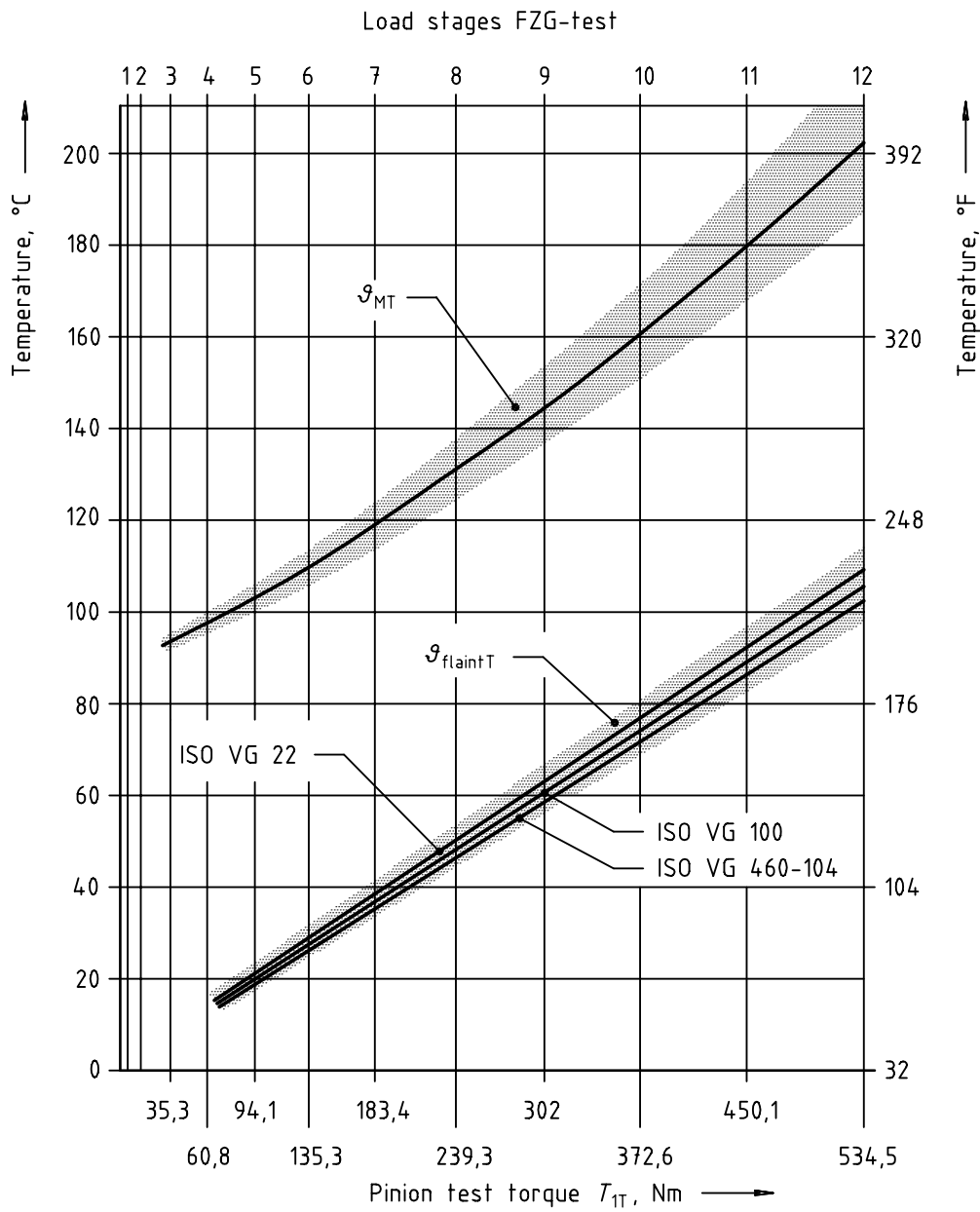


Figure 9 — Scuffing temperature ϑ_{intS} for the FZG test A/8,3/90

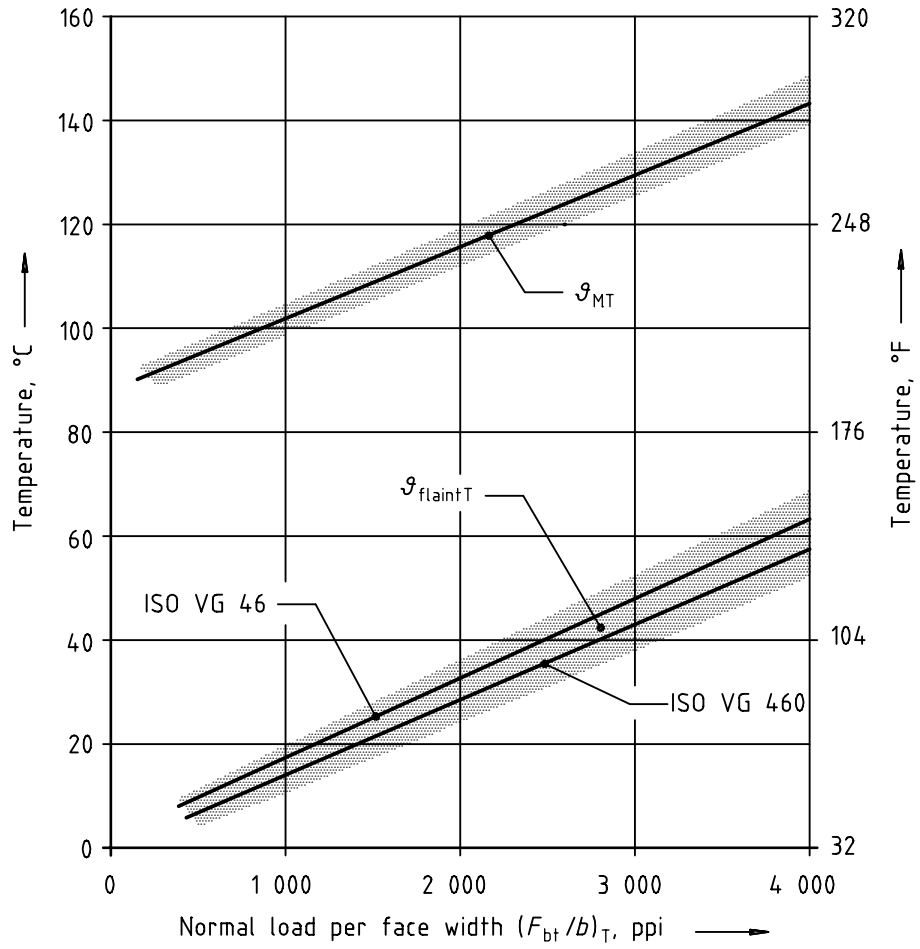


Figure 10 — Scuffing temperature ϑ_{intS} for the Ryder and the FZG-Ryder gear test R/46,5/74

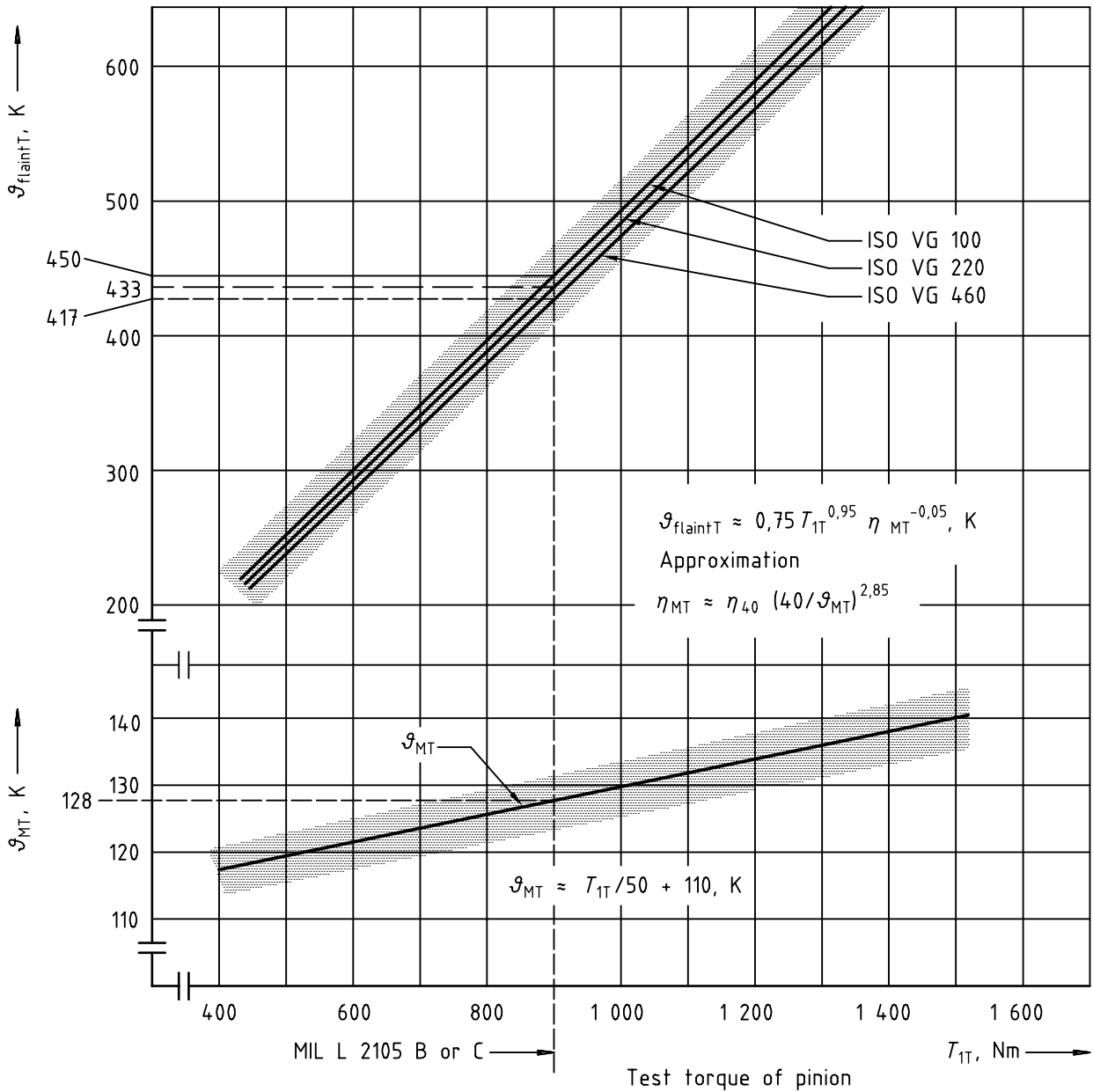


Figure 11 — Scuffing temperature ϑ_{intS} for the FZG L-42 test 141/19,5/110

6.4.2 Relative welding factor X_{WrelT}

The relative welding factor X_{WrelT} is an empirical factor for the influence of the heat treatment or surface treatment on the scuffing integral temperature.

$$X_{WrelT} = \frac{X_W}{X_{WT}} \quad (102)$$

where

$X_{WT} = 1$ for the FZG gear test, the Ryder gear test and the FZG L-42 test;

X_W is the welding factor of the actual gear material as given in Table 3.

Table 3 — Welding factor X_W

Gear material	X_W
Through-hardened steel	1,00
Phosphated steel	1,25
Copper-plated steel	1,50
Bath and gas nitrided steel	1,50
Case carburized steel:	
— average austenite content less than 10 %	1,15
— average austenite content 10 % to 20 %	1,00
— average austenite content greater than 20 % to 30 %	0,85
Austenitic steel (stainless steel)	0,45

Annex A (informative)

Examples

Verifying the accuracy of the integral temperature method the scuffing resistance of the following gear sets was calculated by using the methods according to this part of ISO/TR 13989. The examples contain cylindrical, bevel and hypoid gear drives, with centre distances between $a = 22,07$ mm and $a = 2\,419,63$ mm. The module range includes modules from $m = 1,25$ mm up to $m = 20$ mm. Some of the selected gear units were damaged by a scuffing failure, or near to the scuffing limit (borderline scuffing). In other gear drives no scuffing failure was observed. The data of the gear units and the results of the scuffing calculation are presented in the following tables.

.....

Table A.1 — HELICAL GEAR: Turbine Gear (No. 3 from the Michaelis dissertation)

Description		ISO Symbol	Unit	Value
Number of teeth	pinion	z_1	—	73
	gear	z_2	—	325
Operating centre distance		a	mm	1 419,00
Normal module		m_n	mm	7,000
Normal pressure angle		α_n	°	20,00
Helix angle at standard PD		β	°	11,00
Profile shift factor	pinion	x_1	—	0,010 0
Net face width		b	mm	280,00
Outside diameter	pinion	d_{a1}	mm	534,40
	gear	d_{a2}	mm	2 331,00
Tip relief	pinion	C_{a1}	μm	0
	gear	C_{a2}	μm	0
Index of driving gear		—	—	2
Transmitted power		P	kW	10 295
Pinion speed		n_1	min^{-1}	4 450
Flank surface roughness		R_a	μm	2,00
Tooth root surface roughness		R_z	μm	—
Oil temperature		ϑ_{oil}	°C	40
Lubricant kinematic viscosity at 40 °C		ν_{40}	mm^2/s	32
Scuffing torque in FZG standard test A/8,3/90 according to DIN 51354		T_{1T}	Nm	239
Lubrication factor		X_S	—	1,2
Relative material factor		$X_{W\text{rel}T}$	—	1,00
Run-in factor		X_E	—	1,0
Application factor		K_A	—	1,20
Dynamic factor		K_V	—	1,15
Face load factor		$K_{B\beta}$	—	1,20
Transverse load factor		$K_{B\alpha}$	—	1,10
Coefficient of friction		μ_{mC}	—	0,023
Bulk temperature		ϑ_M	°C	45,6
Integral temperature		ϑ_{int}	°C	55,5
Scuffing safety factor		$S_{\text{int}S}$	—	3,8
Observed failures		No scuffing		

Table A.2 — HELICAL GEAR: Steel Mill Gear (No. 5 from the Michaelis dissertation)

Description		ISO Symbol	Unit	Value
Number of teeth	pinion	z_1	—	28
	gear	z_2	—	28
Operating centre distance		a	mm	580,00
Normal module		m_n	mm	20,000
Normal pressure angle		α_n	°	20,00
Helix angle at standard PD		β	°	10,00
Profile shift factor	pinion	x_1	—	0,303 5
Net face width		b	mm	330,00
Outside diameter	pinion	d_{a1}	mm	619,20
	gear	d_{a2}	mm	619,20
Tip relief	pinion	C_{a1}	µm	0
	gear	C_{a2}	µm	0
Index of driving gear		—	—	1
Transmitted power		P	kW	2 200
Pinion speed		n_1	min ⁻¹	150
Flank surface roughness		R_a	µm	1,50
Tooth root surface roughness		R_z	µm	—
Oil temperature		ϑ_{oil}	°C	32
Lubricant kinematic viscosity at 40 °C		ν_{40}	mm ² /s	220
Scuffing torque in FZG standard test A/8,3/90 according to DIN 51354		T_{1T}	Nm	239
Lubrication factor		X_S	—	1,2
Relative material factor		X_{WrelT}	—	1,00
Run-in factor		X_E	—	1,0
Application factor		K_A	—	1,20
Dynamic factor		K_V	—	1,00
Face load factor		$K_{B\beta}$	—	1,20
Transverse load factor		$K_{B\alpha}$	—	1,00
Coefficient of friction		μ_{mC}	—	0,048
Bulk temperature		ϑ_M	°C	59,6
Integral temperature		ϑ_{int}	°C	109,0
Scuffing safety factor		S_{intS}	—	1,9
Observed failures		No scuffing		

Table A.3 — HELICAL GEAR: Machine Tool Gear (No. 11 from the Michaelis dissertation)

Description		ISO Symbol	Unit	Value
Number of teeth	pinion	z_1	—	5
	gear	z_2	—	28
Operating centre distance		a	mm	22,07
Normal module		m_n	mm	1,250
Normal pressure angle		α_n	°	20,00
Helix angle at standard PD		β	°	20,00
Profile shift factor	pinion	x_1	—	0,350 0
Net face width		b	mm	10,00
Outside diameter	pinion	d_{a1}	mm	9,98
	gear	d_{a2}	mm	38,45
Tip relief	pinion	C_{a1}	μm	0
	gear	C_{a2}	μm	0
Index of driving gear		—	—	1
Transmitted power		P	kW	3,3
Pinion speed		n_1	min^{-1}	15 000
Flank surface roughness		R_a	μm	1,00
Tooth root surface roughness		R_z	μm	—
Oil temperature		ϑ_{oil}	°C	50
Lubricant kinematic viscosity at 40 °C		ν_{40}	mm^2/s	220
Scuffing torque in FZG standard test A/8,3/90 according to DIN 51354		T_{1T}	Nm	450
Lubrication factor		X_S	—	1,0
Relative material factor		X_{WrelT}	—	1,00
Run-in factor		X_E	—	1,0
Application factor		K_A	—	1,00
Dynamic factor		K_V	—	1,00
Face load factor		$K_{B\beta}$	—	1,00
Transverse load factor		$K_{B\alpha}$	—	1,00
Coefficient of friction		μ_{mC}	—	0,144
Bulk temperature		ϑ_M	°C	84,8
Integral temperature		ϑ_{int}	°C	159,4
Scuffing safety factor		S_{intS}	—	2,0
Observed failures		No scuffing		

Table A.4 — HELICAL GEAR: Marine Gear (No. 13 from the Michaelis dissertation)

Description		ISO Symbol	Unit	Value
Number of teeth	pinion	z_1	—	21
	gear	z_2	—	87
Operating centre distance		a	mm	900,00
Normal module		m_n	mm	16,00
Normal pressure angle		α_n	°	20,00
Helix angle at standard PD		β	°	10,00
Profile shift factor	pinion	x_1	—	0,790 0
Net face width		b	mm	370,00
Outside diameter	pinion	d_{a1}	mm	394,50
	gear	d_{a2}	mm	1 465,50
Tip relief	pinion	C_{a1}	µm	0
	gear	C_{a2}	µm	0
Index of driving gear		—	—	1
Transmitted power		P	kW	4 412
Pinion speed		n_1	min ⁻¹	520
Flank surface roughness		R_a	µm	2,00
Tooth root surface roughness		R_z	µm	—
Oil temperature		ϑ_{oil}	°C	60
Lubricant kinematic viscosity at 40 °C		ν_{40}	mm ² /s	150
Scuffing torque in FZG standard test A/8,3/90 according to DIN 51354		T_{1T}	Nm	450
Lubrication factor		X_S	—	1,2
Relative material factor		X_{WrelT}	—	1,00
Run-in factor		X_E	—	1,0
Application factor		K_A	—	1,30
Dynamic factor		K_V	—	1,05
Face load factor		$K_{B\beta}$	—	1,40
Transverse load factor		$K_{B\alpha}$	—	1,00
Coefficient of friction		μ_{mC}	—	0,058
Bulk temperature		ϑ_M	°C	105,1
Integral temperature		ϑ_{int}	°C	185,7
Scuffing safety factor		S_{intS}	—	1,7
Observed failures		Borderline scuffing		

Table A.5 — HELICAL GEAR: Steel Mill Gear (No. 16 from the Michaelis dissertation)

Description		ISO Symbol	Unit	Value
Number of teeth	pinion	z_1	—	24
	gear	z_2	—	79
Operating centre distance		a	mm	700,00
Normal module		m_n	mm	12,00
Normal pressure angle		α_n	°	20,00
Helix angle at standard PD		β	°	27,00
Profile shift factor	pinion	x_1	—	0,550 0
Net face width		b	mm	175,00
Outside diameter	pinion	d_{a1}	mm	360,00
	gear	d_{a2}	mm	1 087,50
Tip relief	pinion	C_{a1}	μm	0
	gear	C_{a2}	μm	0
Index of driving gear		—	—	1
Transmitted power		P	kW	200
Pinion speed		n_1	min^{-1}	240
Flank surface roughness		R_a	μm	2,00
Tooth root surface roughness		R_z	μm	—
Oil temperature		ϑ_{oil}	°C	40
Lubricant kinematic viscosity at 40 °C		ν_{40}	mm^2/s	150
Scuffing torque in FZG standard test A/8,3/90 according to DIN 51354		T_{1T}	Nm	135
Lubrication factor		X_S	—	1,2
Relative material factor		X_{WrelT}	—	1,00
Run-in factor		X_E	—	1,0
Application factor		K_A	—	1,50
Dynamic factor		K_V	—	1,05
Face load factor		$K_{B\beta}$	—	1,40
Transverse load factor		$K_{B\alpha}$	—	1,00
Coefficient of friction		μ_{mC}	—	0,051
Bulk temperature		ϑ_M	°C	48,9
Integral temperature		ϑ_{int}	°C	64,9
Scuffing safety factor		S_{intS}	—	2,3
Observed failures		Borderline scuffing		

Table A.6 — HELICAL GEAR: Turbine Gear (No. 19 from the Michaelis dissertation)

Description		ISO Symbol	Unit	Value
Number of teeth	pinion	z_1	—	43
	gear	z_2	—	44
Operating centre distance		a	mm	161,40
Normal module		m_n	mm	3,628
Normal pressure angle		α_n	°	20,00
Helix angle at standard PD		β	°	12,00
Profile shift factor	pinion	x_1	—	0,000 0
Net face width		b	mm	51,00
Outside diameter	pinion	d_{a1}	mm	166,75
	gear	d_{a2}	mm	170,50
Tip relief	pinion	C_{a1}	µm	40
	gear	C_{a2}	µm	40
Index of driving gear		—	—	1
Transmitted power		P	kW	195
Pinion speed		n_1	min ⁻¹	3 900
Flank surface roughness		R_a	µm	0,75
Tooth root surface roughness		R_z	µm	—
Oil temperature		ϑ_{oil}	°C	70
Lubricant kinematic viscosity at 40 °C		ν_{40}	mm ² /s	68
Scuffing torque in FZG standard test A/8,3/90 according to DIN 51354		T_{1T}	Nm	140
Lubrication factor		X_S	—	1,2
Relative material factor		X_{WrelT}	—	1,00
Run-in factor		X_E	—	1,0
Application factor		K_A	—	1,20
Dynamic factor		K_V	—	1,00
Face load factor		$K_{B\beta}$	—	1,20
Transverse load factor		$K_{B\alpha}$	—	1,00
Coefficient of friction		μ_{mC}	—	0,360
Bulk temperature		ϑ_M	°C	77,7
Integral temperature		ϑ_{int}	°C	91,5
Scuffing safety factor		S_{intS}	—	1,7
Observed failures		Borderline scuffing		

Table A.7 — HELICAL GEAR: Turbine Gear (No. 20 from the Michaelis dissertation)

Description		ISO Symbol	Unit	Value
Number of teeth	pinion	z_1	—	46
	gear	z_2	—	335
Operating centre distance		a	mm	2 419,63
Normal module		m_n	mm	11,000
Normal pressure angle		α_n	°	20,00
Helix angle at standard PD		β	°	30,00
Profile shift factor	pinion	x_1	—	0,000 0
Net face width		b	mm	550,00
Outside diameter	pinion	d_{a1}	mm	606,28
	gear	d_{a2}	mm	4 277,00
Tip relief	pinion	C_{a1}	μm	0
	gear	C_{a2}	μm	0
Index of driving gear		—	—	1
Transmitted power		P	kW	3 153
Pinion speed		n_1	min^{-1}	824
Flank surface roughness		R_a	μm	4,00
Tooth root surface roughness		R_z	μm	—
Oil temperature		ϑ_{oil}	°C	70
Lubricant kinematic viscosity at 40 °C		ν_{40}	mm^2/s	68
Scuffing torque in FZG standard test A/8,3/90 according to DIN 51354		T_{1T}	Nm	61
Lubrication factor		X_S	—	1,2
Relative material factor		$X_{W\text{rel}T}$	—	1,00
Run-in factor		X_E	—	1,0
Application factor		K_A	—	1,30
Dynamic factor		K_V	—	1,20
Face load factor		$K_{B\beta}$	—	1,20
Transverse load factor		$K_{B\alpha}$	—	1,00
Coefficient of friction		μ_{mC}	—	0,033
Bulk temperature		ϑ_M	°C	73,6
Integral temperature		ϑ_{int}	°C	80,1
Scuffing safety factor		$S_{\text{int}S}$	—	1,4
Observed failures		Scuffing		

Table A.8 — SPUR GEAR: Vehicle Gear (No. 25 from the Michaelis dissertation)

Description		ISO Symbol	Unit	Value
Number of teeth	pinion	z_1	—	14
	gear	z_2	—	28
Operating centre distance		a	mm	189,00
Normal module		m_n	mm	9,000
Normal pressure angle		α_n	°	20,00
Helix angle at standard PD		β	°	0,00
Profile shift factor	pinion	x_1	—	0,200 0
Net face width		b	mm	60,00
Outside diameter	pinion	d_{a1}	mm	143,60
	gear	d_{a2}	mm	228,00
Tip relief	pinion	C_{a1}	μm	0
	gear	C_{a2}	μm	0
Index of driving gear		—	—	1
Transmitted power		P	kW	410
Pinion speed		n_1	min^{-1}	1 300
Flank surface roughness		R_a	μm	0,80
Tooth root surface roughness		R_z	μm	—
Oil temperature		ϑ_{oil}	°C	100
Lubricant kinematic viscosity at 40 °C		ν_{40}	mm^2/s	220
Scuffing torque in FZG standard test A/8,3/90 according to DIN 51354		T_{1T}	Nm	372
Lubrication factor		X_S	—	1,0
Relative material factor		X_{WrelT}	—	1,00
Run-in factor		X_E	—	1,0
Application factor		K_A	—	1,30
Dynamic factor		K_V	—	1,00
Face load factor		$K_{B\beta}$	—	1,20
Transverse load factor		$K_{B\alpha}$	—	1,00
Coefficient of friction		μ_{mC}	—	0,073
Bulk temperature		ϑ_M	°C	158,3
Integral temperature		ϑ_{int}	°C	283,2
Scuffing safety factor		S_{intS}	—	1,0
Observed failures		Scuffing		

Table A.9 — Bevel and hypoid gears

Description	ISO Symbol	Unit	Test gear 1	Test gear 2	Test gear 3	Test gear 4	
Pinion offset	a	mm	0	25,4	44	44	
Number of teeth	pinion	z_1	—	8	10	11	12
	gear	z_2	—	35	41	41	45
Normal module	m_n	mm	3,350	3,070	3,280	3,400	
Normal pressure angle	α_n	°	16,00	20,00	19,00	19,00	
Normal pressure angle	α_{nZ}	°	16,00	20,00	19,00	19,00	
Normal pressure angle	α_{ns}	°	16,00	16,60	9,00	12,75	
Mean helix angle	pinion	β_{m1}	°	37,50	50,40	52,10	50,68
	gear	β_{m2}	°	37,50	31,40	18,00	21,10
Pitch cone angle	pinion	δ_1	°	12,88	14,33	16,85	20,32
	gear	δ_2	°	77,10	75,23	69,90	66,93
Profile shift factor	pinion	x_{m1}	—	0,600 0	0,740 0	0,770 0	0,500 0
Net face width		b_2	mm	28,00	28,00	25,00	25,40
Outside diameter	pinion	d_{am1}	mm	44,30	58,50	69,90	73,74
	gear	d_{am2}	mm	148,50	148,10	142,00	165,40
Index of driving gear	—	—	1	1	1	1	
Pinion test torque	T_1	Nm	520	300	230	670	
Pinion speed	n_1	min ⁻¹	4 500	4 500	4 500	4 500	
Flank surface roughness	Ra	µm	0,24	0,24	0,62	0,30	
Oil temperature	ϑ_{oil}	°C	90	90	90	180	
Lubricant kinematic viscosity at 40 °C	ν_{40}	mm ² /s	220	220	220	220	
Scuffing torque in FZG standard test A/8,3/90 according to DIN 51354	T_{1T}	Nm	450	450	450	> 534 ^a	
Lubrication factor	X_S	—	1,0	1,0	1,0	1,0	
Relative material factor	X_{WrelT}	—	1,25	1,25	1,25	1,25	
Run-in factor	X_E	—	1,0	1,0	1,0	1,0	
Application factor	K_A	—	1,00	1,00	1,00	1,00	
Coefficient of friction	μ_{mC}	—	0,097	0,053	0,065	0,063	
Bulk temperature	ϑ_M	°C	214,3	166,1	204,7	337,9	
Integral temperature	ϑ_{int}	°C	480,7	361,8	499,7	743,8	
Scuffing safety factor	S_{intS}	—	0,7	1,0	0,7	1,2	
Observed failure	—	—	Scuffing	Scuffing	Scuffing	No scuffing	

NOTE Test gears 1, 2 and 3 were taken from:

Richter, M.: Der Verzahnungswirkungsgrad und die Fresstragfähigkeit von Hypoid- und Schraubenradgetrieben. Diss. TU München (1976).

Test gear 4 is used in the scuffing test "FZG-Hypoidöltest Form A".

^a Test oil meets API GL-5 specification.

Annex B (informative)

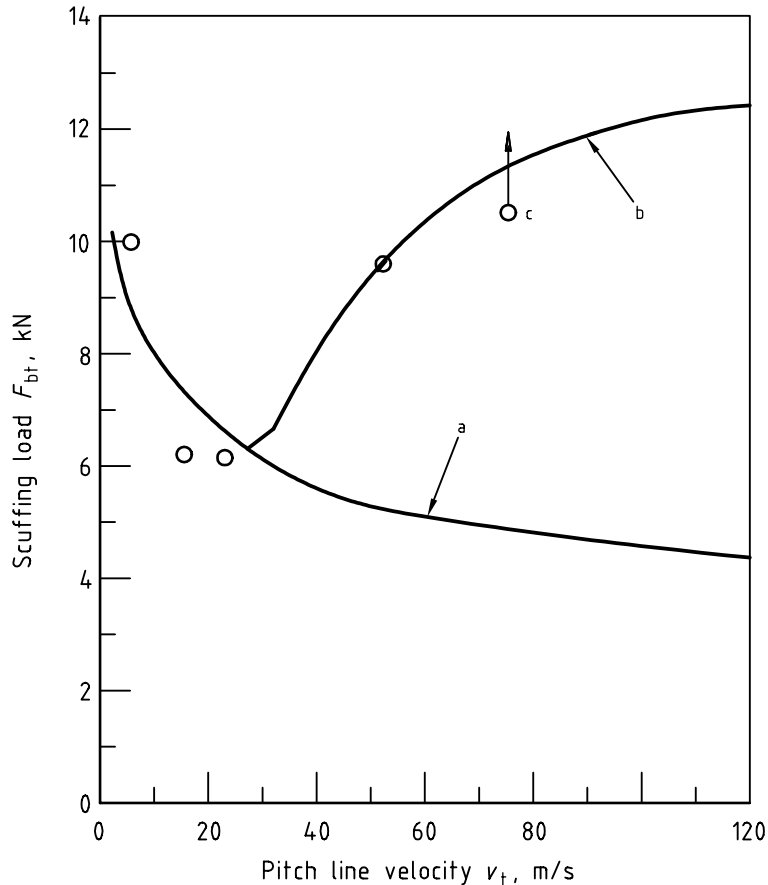
Contact-time-dependent scuffing temperature

This annex describes the method of using a variable scuffing temperature ϑ_S for CTC (Contact-Time Criterion) according to [6].

The actual calculation methods of a critical value which must not be exceeded are

- the maximum local and instantaneous total contact temperature ϑ_S ;
- the mean weighted surface temperature across the contact ϑ_{intS} .

These limits are assumed to be independent of speed, so the scuffing load decreases with load up to highest speeds. Therefore the calculation of gears lubricated with EP-oils is very conservative at high speed (Figure B.1).

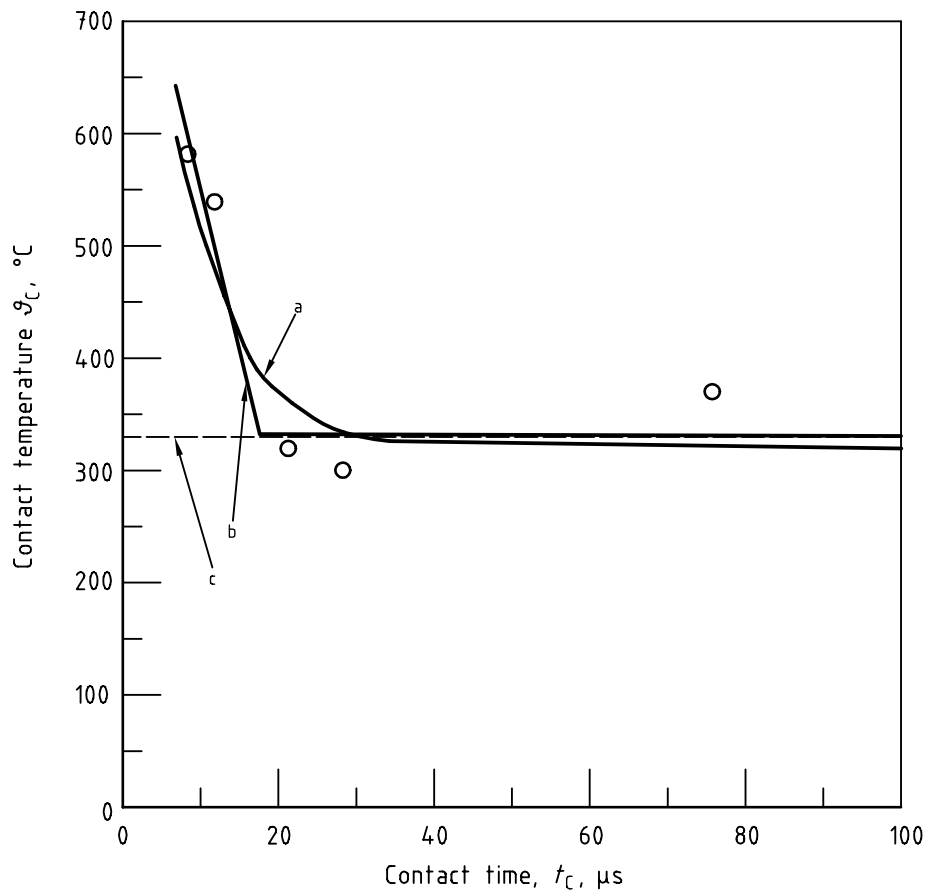


Key

- o Test results, A-type gears, oil Z49
- a Curve a: calculation with constant critical temperature according to Figure B.2, curve c
- b Curve b: calculation with time dependent critical temperature ϑ_S according to Figure B.2, curve b
- c No damage

Figure B.1 — Dependency of scuffing load on speed

To improve the calculation method at high speeds, as well as contact points close to the base circle, the fact has to be considered that the critical temperature ϑ_S is dependent on the contact time t_C . Figure B2 shows an example. The calculated curve (a) according to [6] is approximated by two straight lines (b). This modification of the CTC-method gives the required result: The calculated and the measured scuffing load are close together.



Key

- Test results, A-type gears, oil Z49
- a Curve a: calculated critical temperature
- b Curve b: approximation of curve a
- c Curve c: critical temperature

Figure B.2 — Influence of contact time t_C on the critical contact temperature

The dependence of the scuffing temperature ϑ_S on the contact time t_C is approximated as shown in Figure B.2 by two straight lines:

$$\vartheta_S = \begin{cases} \vartheta_{SC} & \text{for } t_C \geq t_K \\ \vartheta_{SC} + C_S \cdot X_{WrelIT} \cdot (t_K - t_C) & \text{for } t_C < t_K \end{cases} \quad (\text{B.1})$$

where

ϑ_S is the scuffing temperature;

ϑ_{SC} is the constant scuffing temperature at long contact times, which corresponds to ϑ_S of CTC;

t_C is the contact time;

t_K is the contact time at the minimum of the scuffing-speed-curve;

C_S is the gradient of the scuffing temperature;

X_{WrelT} is the relative welding factor.

C_S and t_K have to be determined by two oil tests at short contact times (high speed). The contact times in the tests should be in the range of 20 μ s.

t_C and C_S is calculated as follows (the indices describe the tests at low, middle and high velocity):

$$t_K = \frac{(\vartheta_{Bm} - \vartheta_{SC}) \cdot (t_{Cm} - t_{Cf})}{\vartheta_{Bf} - \vartheta_{Bm}} + t_{Cm} \quad (B.2)$$

$$C_S = \frac{\vartheta_{Bf} - \vartheta_{Bm}}{t_{Cm} - t_{Cf}} \quad (B.3)$$

There is a constant value of the scuffing temperature (in the range of long contact times).

$$\vartheta_{SC} = \vartheta_1 \quad (B.4)$$

t_C is the time that one point of the gear flank (pinion of wheel) needs to cross the Hertzian contact width ($2 \cdot b_H$).

$$t_{C1} = \frac{2 \cdot b_H}{v_1} \quad (B.5)$$

$$t_{C2} = \frac{2 \cdot b_H}{v_2} \quad (B.6)$$

$$t_C = \min(t_{C1}, t_{C2}) \quad (B.7)$$

where v_1 and v_2 are the surface velocity of pinion and wheel, respectively.

If there are no oil test results available at high speeds, the scuffing temperature ϑ_S can be approximated by the following recommendation.

a) Non-EP-oils:

The increase of the critical temperature at high velocities is very low. Therefore the calculation is made with a constant scuffing temperature ϑ_{SC} .

b) EP-oils:

It is proposed to use the following values of t_K and C_S :

$$t_K = 18 \mu\text{s}$$

$$C_S = 18 \text{ K}/\mu\text{s}$$

For the scuffing temperature ϑ_S the equation reads:

$$\vartheta_S = \begin{cases} \vartheta_{SC} & \text{for } t_C \geq 18 \mu\text{s} \\ \vartheta_{SC} + 18 \cdot X_{WrelT} \cdot (18 - t_C) & \text{for } t_C < 18 \mu\text{s} \end{cases} \quad (B.8)$$

ϑ_{SC} has to be determined in a scuffing oil test, i.e. the FZG-test A/8,3/90 according to DIN 51354 [2].

Determination of tangential velocity and Hertzian contact width in cylindrical gears:

Tangential velocities at the flank:

$$v_1 = \rho_1 \cdot \omega_1 = \rho_1 \cdot \frac{2 \cdot \pi \cdot n_1}{60} \quad (\text{B.9})$$

$$v_2 = \rho_2 \cdot \omega_2 \quad (\text{B.10})$$

Hertzian contact width (same Young's Modulus of pinion and wheel, line contact):

$$2 \cdot b_H = 3,04 \cdot \sqrt{\frac{F_{bt}}{b \cdot E} \cdot \frac{\rho_1 \cdot \rho_2}{\rho_1 + \rho_2}} \quad (\text{B.11})$$

© ISO 2000. All rights reserved.

Bibliography

- [1] Michaelis, K. Die Integraltemperatur zur Beurteilung der Freßtragfähigkeit von Stirnradgetrieben. Diss. TU München 1987.
- [2] DIN 51354, FZG-Zahnrad-Verspannungsprüfmaschine, Prüfverfahren A/8,3/90 für Schmieröle.
- [3] Federal Test Method Std. No. 791 B, Method 6508.1: Load Carrying Capacity of Lubricating Oils (Ryder Gear Machine).
- [4] Winter, H., Michaelis, K., Funck, G. Der FZG-Ryder-Freßtest für Flugturbinenschmierstoffe. Tribologie + Schmierungstechnik 35 (1988) H. 1, S. 30-37.
- [5] Michaelis, K. Freßtragfähigkeit für Hochleistungs-Hypoidgetriebe-Schmierstoffe. Mineralöltechnik 23 (1978) Nr. 13, S. 1-24.
- [6] Collenberg, H.F. Untersuchungen zur Freßtragfähigkeit schnelllaufender Stirnradgetriebe. Diss. TU München 1991.
- [7] Dubbel. Taschenbuch für den Maschinenbau, 16. Auflage, Springer Verlag Berlin, Heidelberg, New York, London, Paris, Tokyo (1987).
- [8] Lechner, G. Die Freß-Grenzlast bei Stirnrädern aus Stahl. Diss. TH München 1966.
- [9] Ishikawa, J., Hayashi, K., Yokoyama, M. Surface Temperature and Scoring Resistance of Heavy-Duty Gears. Inst. of Technology, Tokyo 1972.
- [10] Grekoussis, R., Michailidis, Th. Näherungsgleichungen zur Nach- und Entwurfsrechnung der Punktberührung nach Hertz. Konstruktion 33 (1981).

ICS 21.200

Price based on 48 pages